HELSINKI UNIVERSITY OF TECHNOLOGY
Faculty of Electronics, Communications and Automation
Department of Radio Science and Engineering

Alberto Blasco

COMPARISON OF SNOW-COVERED AREA ESTIMATION METHODS IN NORTHERN FINLAND

Supervisor: Licentiate of Science in Technology Kari Luojus

Espoo, 15 of July 2008

Preface

The work presented in this Final Project has been carried out in the Laboratory of Space Technology at Helsinki University of Technology under the supervision of Licentiate of Science in Technology Kari Luojus.

I want to thank Kari Luojus for teaching and introducing me into the snow remote sensing field and especially for assistance and supervising me during the whole process of this work. I am also grateful for the contribution and means of the TKK University of Technology and especially to the Laboratory of Space Technology that made this work possible.

I would like to express my best sincere gratitude to my family, for their moral and economical support during all my studies and especially for giving me encouragement to finish them as an exchange student, my mother and father, Mª Concepcion Cutrona and Francisco Blasco, my sister Elsa Blasco, and my grandmother Josefa Benavent.

I am also grateful to the friends who I have been sharing these last months as an exchange student facilitating me to improve my english skills, and overall, to my office mate Marc Mir, who helped me during the development of this Final Project.

Finally, I really want to thank William Martin for all the scientific writing support, correcting and revising of all the steps during the writing process of this work.

Abstract

Author: Alberto Blasco Cutrona

Name of the Project:
Comparison of snow-covered area estimation methods in northern Finland

Date: 15 of July 2008

Number of Pages: 81

Department:
Faculty of Electronics, Communications and Automation
Department of Radio Science and Engineering

Professorship: Space Technology

Supervisor: Licentiate of Science in Technology Kari Luojus

Abstract:

An accuracy evaluation of the Nagler & Rott snow-covered area estimation method is presented in this work. The main objective is to determinate the effects of the threshold level, the reference image, as well as the area analysed.

The method is studied by conducting the SCA estimation for 14 Radarsat intensity images of northern Finland where is dominated by boreal forest. The results are also compared with the estimations carried out by the current TKK method.

Keywords:

Remote sensing, Snow Covered Area, Thomas Nagler, Helmut Rott, backscattering, Radarsat, threshold, Radar

Resumen

Desde hace muchos años, mejorar las previsiones meteorológicas y la monitorización del comportamiento climático ha sido uno de los principales objetivos de los institutos meteorológicos. No obstante, los sistemas tradicionales de medida se han visto desbordados por la necesidad de cubrir amplias áreas de terreno con la mayor brevedad posible, dando paso al desarrollo de nuevas tecnologías. En este aspecto, la teledetección espacial (Remote sensing) mediante satélites es uno de los campos que ha experimentado una mayor evolución en múltiples aplicaciones y sistemas. La razón es simple, permite cubrir miles de kilómetros cuadrados en una única imagen, y monitorizar la evolución medioambiental repitiendo la adquisición en un intervalo de tan solo días.

El norte de Finlandia, con un área superior a los 100000 km^2, está dominado durante más de una tercera parte del año por condiciones hibernales. Normalmente estas áreas se encuentran cubiertas por un amplio espesor de nieve volviéndose agua al final de periodo de deshielo. Esto supone unas importantes reservas hidrológicas por lo que monitorizar este proceso facilita las operaciones de las industrias hidroeléctricas, la previsión de inundaciones así como las previsiones meteorológicas y la monitorización del medio ambiente. Actualmente los sistemas de teledetección basados en sensores ópticos ya son utilizados en esta región para predecir la superficie cubierta por nieve (snow-covered area), realizando estimaciones de alta precisión. Sin embargo, estos sistemas requieren de visibilidad directa y luz solar en el momento de la adquisición, por lo que raramente son capaces de cubrir el 100% del área. No obstante, los sistemas basados en Radar (como los comparados en este proyecto final de carrera) permiten realizar estás estimaciones incluso con nubosidad o de noche, aunque a cambio no alcanzan un nivel tan alto de exactitud.

La teledetección basada en Radar, tiene como objetivo predecir la naturaleza de la superficie terrestre basándose en las características de la radiación electromagnética recibida después de reflejarse en el suelo. La detección de superficies cubiertas por nieve ha conducido una de las importantes ramas dentro de este campo, donde los valores de backscattering están influenciados por la humedad y tamaño del grano así como también por el volumen de nieve. La principal aplicación en este campo es la monitorización de la época de deshielo durante la cual los valores de backscattering siguen una tendencia decreciente debido al aumento del contenido líquido de la nieve.

El objetivo principal de este proyecto final de carrera es analizar y comparar la exactitud de un método de predicción de superficies nevadas importado a una zona para la cual no ha sido diseñado. Se trata del método desarrollado por Nagler & Rott diseñado para funcionar en los Alpes, en zonas con una topografía abrupta y con una vegetación poco densa aplicado a las regiones del norte de Finlandia, una área con una topografía plana y abundantes bosques

boreales. El principal cálculo sobre el que se basa este método es la comparación de niveles de potencia entre la imagen analizada y una utilizada como referencia. Cuando la diferencia entre ambas potencias es menor que un cierto valor de threshold se considera que el pixel se corresponde con un área no cubierta por nieve y viceversa, obteniendo un valor de tanto por ciento de superficie nevada para cada sub-área después de promediar el total de pixels dentro de dicha área. El proceso de evaluación y análisis de este método permite determinar que valores de threshold permiten obtener los mejores resultados y los factores que afectan a la exactitud de las estimaciones en esta región, permitiendo el desarrollo de un sistema adaptado al norte de Finlandia basado en el algoritmo de Nagler & Rott. Los resultados son comparados a su vez con el método desarrollado en la Universidad Tecnológica de Helsinki (TKK) ampliamente mejorado para funcionar en esta región.

Los datos utilizados en este proyecto fueron adquiridos mediante Radar de apertura sintética a través del satélite Radarsat. La resolución de las imagenes es de 100m x 100m y cubren un área superior a los 500km x 500km. Las 14 imagenes procesadas corresponden a las sesiones de deshielo del 2004 al 2006 todas ellas entre los meses de marzo y mayo. Cada imagen en los análisis está dividida a su vez en 2037 sub-áreas correspondientes, según el Watershed Simulation and Forecasting System (WSFS),con las cuencas de desagüe.

En los dos métodos comparados, las imagenes de referencia son una de las partes más importantes en el proceso de estimación. Estas imagenes corresponden con el momento en el que los valores de backscattering son más elevados, siendo en el principio (nieve seca) o el final (suelo sin nieve) de la sesión de deshielo. Se utilizan para tener unos valores de referencia de la misma área geográfica, que son utilizados luego para realizar las estimaciones. El primer punto del análisis tiene como objetivo determinar cual de las 4 imagenes elegidas como referencia genera los mejores resultados y para que valores de threshold. Además, se analizan los resultados para tres tipos de áreas; abiertas, cubiertas por bosque y la combinación de ambas.

Continuando con el análisis, el siguiente punto contemplado es extrapolar los valores de threshold que generan los mejores resultados, utilizando el conjunto completo de imagenes, a una sola imagen. Esta evaluación permite comprobar que es necesario determinar los valores de threshold independientemente para cada imagen y que además siguen una tendencia relacionada con el momento, dentro de la sesión de deshielo, en el que fue adquirida la imagen.

El siguiente punto evalúa la influencia de la amplia área cubierta por cada imagen, demostrando que la utilización de un único valor de threshold para cubrir toda la región del norte de Finlandia reduce la exactitud de las predicciones. Esto es debido, principalmente, a que las regiones más norteñas se encuentran en un momento distinto dentro del proceso de deshielo que las regiones sureñas. La conclusión obtenida en este punto, es que es necesario dividir el área en al menos 5 sub-áreas de menor tamaño.

Finalmente, un Nuevo método basado en el algoritmo desarrollado por Nagler & Rott adaptado al norte de Finlandia es desarrollado partiendo de las principales conclusiones obtenidas mediante el proceso de análisis. En el último apartado los resultados obtenidos con el Nuevo método adaptado son comparados con el actual método diseñado en la TKK.

Index

List of Acronyms and Symbols

CEOS	*Committee on Earth Observation Satellites*
DEM	*Digital Elevation Model*
ERS-2	*European Remote Sensing Satellite-2*
ESA	*European Space Agency*
TKK	*Helsinki University of Technology*
MAE	*Mean Absolute Error*
MODIS	*Moderate-resolution Imaging Spectroradiometer*
NDVI	*Normalized Difference Vegetation Index*
RADAR	*Radio Detection and Ranging*
RMSE	*Root Mean Squared Error*
SAR	*Synthetic Aperture Radar*
SCA	*Snow-Covered Area*
SCW	*ScanSAR Wide A*
SNWC	*Snow liquid Water Content*
SYKE	*Finnish Environment Institute*
TIFF	*Tagged Image File Format*
TR	*Threshold*
WSFS	*Watershed Simulation and Forecasting System*
WSA	*Weather Station Assimilation*

θ	angle of incidence in relation to the reference surface
λ	wavelength
σ^o	radar backscattering coefficient
σ^o_{can}	forest canopy backscattering contribution
$\sigma^o_{ground,\ ref}$	reference backscattering coefficient from the snow-free ground
$\sigma^o_{ground,\ snow}$	reference backscattering coefficient from the wet snow-covered ground
σ^o_{surf}	backscattering coefficient of the ground or snow layer
σ^o_{ws}	backscattering coefficient ot the wet snow covered ground
σ^o_{ref}	reference backscattering coefficient from the snow-free or dry snow
$\rho_{\lambda,obs}$	observed reflectance at λ wavelength
$\rho_{\lambda,forest}$	applicable reflectance for dense coniferous canopies at λ wavelength
$\rho_{\lambda,ground}$	applicable reflectance for snow-free ground at λ wavelength
$\rho_{\lambda,snow}$	applicable reflectance for wet snow at λ wavelength

a	constant coefficient, describing canopy extinction coefficient
A_{ill}	cross-area of illuminated target
c	the speed of light
f	frequency
G_n	antenna gain
L	autocorrelation length
m	surface slope
n	amount of samples

P_r	received power
P_t	transmitted power
r’	distance between object and antenna
t^2	two-way transmittivity through the forest canopy
s	standard deviation of wet snow surface height
V	forest stem volume
x_i	estimated value
y	reference value
y_i	reference value

1 Introduction

For many years now, the forecast and monitoring of environmental behaviour has been one of the priorities of the meteorological institutes, which has led to evolution of the employed means. Usually, the traditional ways of collecting ground-based information are not able to cover large geographical areas in short time periods, and are also typically very expensive. Fortunately, the high technological development has provided good ways to improve these different methods presenting newer alternatives. Right from the first satellite launch in the 1960s until the present day, many investigations have been carried out in remote sensing field based on satellite data. The reason is simple, it enables the monitoring of large areas using only one image and repeating this acquisition process at daily intervals with access to the data shortly after the satellite overpass.

Northern Finland, covering a large area of more than 100000 km^2, is dominated by winter conditions for more than one third of the year. Typically, these areas are covered with deep snow during this period that becomes water after the melting season. The hydrological potential of these annual reserves is significant; therefore their monitoring facilitates the hydropower industry operations, prevention of floods, as well as the weather forecasting and environmental monitoring. In recent years, optical remote sensing by satellites has been used to predict the snow covered area (SCA) during the melting season, monitoring this process with a high degree of accuracy. This method is based on the high reflectance of snow in the working range of wavelengths, but is not always available. Both sufficient Sunlight and cloud-free conditions are required at the acquisition moment and rarely reach 100% of area coverage in these estimates. Therefore, as alternative other methods have been developed based on Radar remote sensing data for the unavailable optical data. The main advantage of those is the capacity to acquire data even when the optical remote sensing is inhibited. The current Radar based methods, however, are slightly less accurate and significantly more expensive than the optical methods.

Remote sensing, in all the fields applied, has as objective to predict the nature of the earth surface based on the characteristics of the electromagnetic radiation received by the sensor that is scatter from the ground surface. This is possible because the features of the emitted waves change when they interact with the different mediums. In the detection of snow surfaces the backscattering values are influenced by snow wetness, grain size, and snow pack structure. The grain size is largest in the dry snow situation, and as a consequence remains transparent without interfering with the electromagnetic wave resulting as the bare ground coefficients. Once the melt season starts, the snow becomes wet reducing the backscattering level. Estimating the evolution of this process is possible by analysing the progressive variation of these coefficients for the different locations during the melting process. SCA maps can be obtained by analysing the backscattering signatures.

The satellite data used in this study is acquired by synthetic aperture radar (Section 2.1) which presents important advantages in the remote sensing of large areas. The Radarsat system has been designed to achieve high spatial resolutions (from 5 to 100 meters on C-band) covering areas up to 500km x 500km. Furthermore, the temporal resolution is typically less than one week and depends on the latitude, imaging mode and sensor; an image can be available every day in high latitudes. In conclusion, this system is good for environmental monitoring because of the large area coverage at high temporal resolution.

The Helsinki University of Technology (TKK) SCA method has been developed during the last years achieving great results. The method has been designed to make estimates taking into account effect of boreal forest and the modest topography dominant in this region, using also the information from the weather stations to avoid false results. This method is briefly explained in Section 2.5 [2]. The purpose of this Final Project is to adapt and evaluate the algorithm explained by Nagler & Rott (Section 2.7) [1] implemented and tested on the mountainous areas in the Eastern Alps of Austria. The main objectives are to assess the accuracy of the method for the complete SAR data set available for the years 2004 to 2006, and to evaluate the different variables affecting the results.

The second chapter presents all the theoretical background, the test site and data features are explained in the third chapter. Finally, the process to assess the results and the complete evaluations are included on the fourth chapter. The summary and the main conclusions are listed in the fifth chapter.

2 Theory and Methods

2.1 Synthetic Aperture Radar system

Synthetic aperture radar (SAR) works over the basics of Radio Detection and Ranging (Radar) systems inside the microwaves range of frequency. In other words, the use of electromagnetic waves to identify range, altitude, direction and also the speed of moving as well as fixed objects. SAR instead of typical Radar incorporates a sophisticated post-processing of radar data used to produce a very narrow effective beam. It has been used by moving instruments like satellites or planes over relatively immobile targets where the main applications are remote sensing and mapping.

The operation of Radar systems is based on sending radio frequency signals and measuring the backscattered signal produced by the objects in the propagation path of the transmitted signal. These values change, depending on the features of the object or surface analysed, and consequently can be used to identify it. The backscattering rate is calculated with the next equation [5]:

$$\sigma^{\circ} = \frac{P_r (4\pi)^3}{P_t \lambda^2} \cdot \frac{1}{\int_{Aill} \frac{G_n^2}{r^4}} \approx \frac{P_r (4\pi)^3}{P_t \lambda^2 G^2} \frac{r'^4}{A'_{ill}} \qquad (1)$$

Where the main rate is Pr (received power) divided by Pt (transmitted power). The backscattering value is also affected by λ (wavelength), G (antenna gain), r' (distance between object and antenna) and A'ill (illuminated area).

The most important advantage of SAR is that it uses the movement of the satellite platform to take many samples of the same target from different points. As a result the antenna works as a virtual antenna with a greater aperture size. The amount of measurements acquired for each target is dependent on the size of the synthetic aperture, and as a consequence, the resolution acquired is similar to a real aperture antenna of the same size.

The resolution of the SAR images is split into two dimensions where each one is independent of the other. The azimuth is the direction followed by the satellite and the slant range is the direction perpendicular to the line of flight. Therefore the range resolution is directly related to the bandwidth of the transmitted pulse: the positions of the received signals are shifted in space by measuring the time differences between them (more delay for farther distance). On the other hand, the identification across the azimuth direction is calculated by referring to the

Doppler frequency which requires the motion of the spacecraft. Each acquired signal is located, in relation to the satellite, at a specific angle that changes over time.

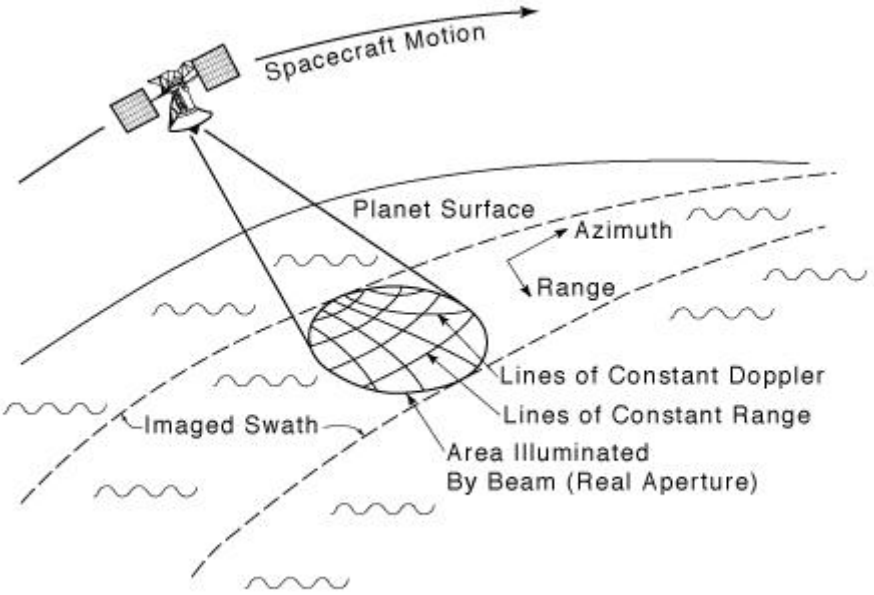

Figure 1, Synthetic aperture radar operation

The format of the data is a two dimensional matrix with values for each pixel corresponding to the backscattering level registered for each resolution point. Once the data has been acquired, it can be processed depending on the application with the most suitable algorithm in order to interpret the results. It is possible then to render accurate maps even without cloud-free conditions or direct visibility.

2.2 The Radarsat-1 Satellite

All the satellite data used for snow-covered area estimation in this study was acquired by Radarsat-1, the first Canadian Earth observation Satellite launched in November of 1995. It works along a sun-synchronous orbit above the earth where the observations of the same point are always at the same local solar time. It orbits at an altitude of 798 kilometres with an inclination of 98.6 degrees. Radarsat-1 has an orbital period of 100.7 minutes, meaning that it circles the Earth 14 times a day, the satellite reaches the same position relative to earth every 24 days.

The Radarsat SAR operates in the microwave frequency range of C-band with a frequency of 5.3 GHz, which is able to penetrate clouds and precipitation. Moreover, it transmits and receives in horizontal polarization (HH).

Radarsat-1 was designed with seven SAR imaging modes or beam modes. In short, each one offers different area coverage (from 50x50 km to 500x500 km) and as a consequence, changes the resolution ensuring that it is the same in both range and azimuth (from 8 m to 100 m). In addition, it is also possible to choose the incidence angles from a range (10° - 59°).

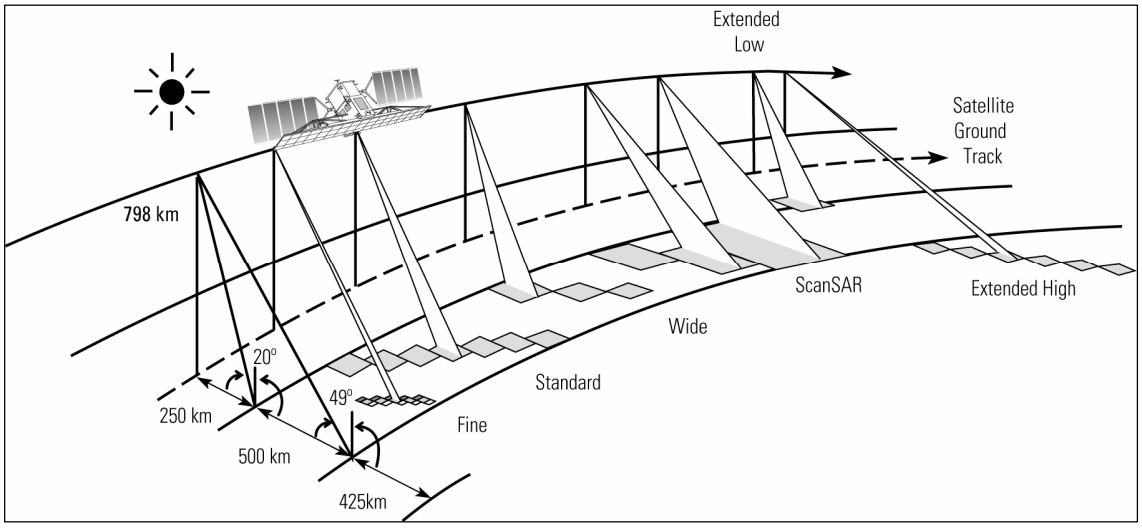

Figure 2, Radarsat-1 operation modes

2.3 Remote Sensing of Snow Surfaces

The term `remote sensing´ refers to the gathering of information about an object without direct physical contact, and more precisely when this acquisition is via airbone or spaceborn observations using electromagnetic radiation. Usually these signals cover long distances being necessary the transmission using the microwave frequency range (Radarsat operates at 5.3 Ghz) which allows the highest directivity and, consequently, better signal level in reception. Essentially, the predictions about the nature of the earth surface are based on the characteristics of the backscattering received by the sensor from the ground. It is possible because the properties of the materials and their effects on the signals are well known.

The SCA (Snow-Covered Area) estimation is a variable used to approximate the percentage of area covered by snow. It can be determined from backscattering data received. Many algorithms have been developed to cover large areas, by satellite data, obtaining important information for hydrological monitoring systems. Instead of optical remote sensing, SAR (Synthetic Aperture Radar) images can be used in all weather conditions and also at night. However, the accuracy of these estimates is usually not as good as those obtained using optical data. The relevant electromagnetic interactions are complicated in snow detection using radar data, because generally dry snow remains transparent to radar unless the snow pack is very deep, and then the results are approximately equivalent to those of bare ground. Nevertheless, when the liquid water content of snow exceeds about 1%, the physical properties start to change and the backscattering starts to be dominated by surface scattering. In this respect, it has been demonstrated in various studies that wet snow cover can be distinguished from snow free terrain because wet snow has low level of backscattering compared to dry snow or bare ground (Rott 1984; Hallikainen et al. 1992; Rott and Nagler 1995; Baghdadi, Fortin, and Bernier 1999; Rees and Steel 2001). Therefore, is possible to monitor the melting periods looking at the behaviour of the backscattering signature. Typically, the amount of backscattering increases because the amount of bare ground increases during the melting process, as shown Figure 3:

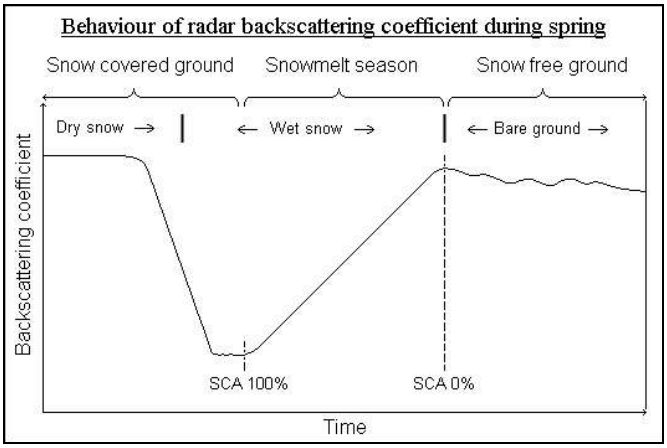

Figure 3, the Behaviour of the backscattering coefficient during the snow melt season

R. Magagi and M. Bernier conducted, in Canada, an interesting experiment about the variables which affect the value of Radarsat backscattering data during the snow melting season. It was done by comparing the snow-field measurements with the Satellite data, both acquired on the same days. The main goal of this study was to investigate the optimal threshold level in order to discriminate between dry snow and wet snow surfaces, and evaluate if the reported [1] -3dB threshold value is feasible for wet snow detection.

The principal field-measurements were about the snow density, grain size, volumetric liquid water content, and temperature along several profiles at different locations. Both dry snow and wet snow conditions were analysed in order to determine their main features. The soil and snow roughness was estimated using three sources: the Radarsat data measured in the snow-free conditions, the Radarsat images under study, and the bare soil signal simulated from the Integral Equation Method [3]. The backscattering averaged values for the dry snow images and for the wet snow images, showed only a -1dB difference within the 45°- 49° incidence angle range, corresponding to the S7 beam mode. The next point investigated the variation in the signal partition with the changes of snow surface wetness and roughness in order to be able to estimate the relationship between wet snow and dry snow signals.

The differences between the main contributions in the total backscattering level for each one of the situations were noted. The dry snow cover information: satellite images, field-measurements and simulations, from several incidences angles, showed that the signal corresponding to the snow-ground interface dominates the scattering processes, for all the angles, whereas the air-snow interface provides the least contribution. On the other hand, the wet snow cover presented other peculiarities. The importance of the scattering level resulting from the volume for smooth wet snow was noted, also for low values of snow liquid water content and at high incidence angles. In both standard modes S1 (23°) and S7 (47°) the contribution at the air-snow interface increases when the surface slope increase and becomes more significant than the volume level. In summary, the study concluded: if a wet snow cover has low snow liquid water content and also high roughness, the global backscattering level could increases up to the backscattering value measured for a dry snow surface, being impossible to discriminate by looking simply at the threshold level.

The relationship between all of these variables were plotted in the Figure 4 for each one of the beam modes, where the vertical line marks the limit of the minimum snow liquid water content, and the horizontal line marks the -3dB threshold level used in several algorithms. Each one of the representations is related with a surface slope defined by:

$$m = \sqrt{2} * (s / L) \qquad (1)$$

Where s (cm) is the estimated value of the standard deviation of the wet snow surface height and L (cm) is the autocorrelation length.

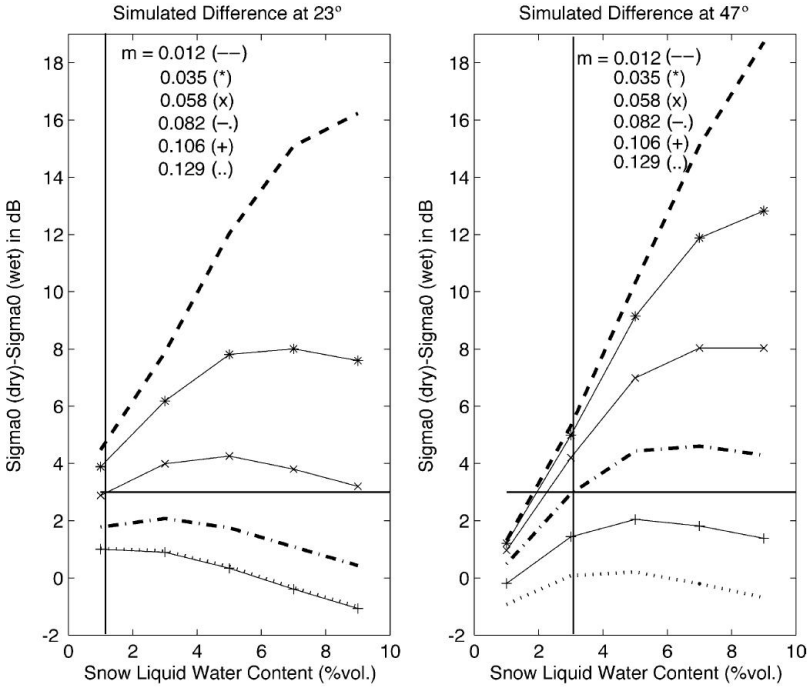

Figure 4, Difference between the dry snow signals and the modeled wet snow backscattering coefficients as a function of the volumetric snow surface liquid water content, snwc (vol.%), and for several values of the wet snow surface slope, m, in the standard modes S1 and S7. The horizontal and vertical lines delimit the optimal conditions in wet snow surface roughness and liquid water content values, respectively.

2.5 TKK Method for Snow-Covered Area Estimation

The Snow-Covered Area (SCA) estimation method developed at TKK uses the SAR data, acquired by ERS-1/2 or the Radarsat, to generate estimates during the snow melting process. The complete estimate involves eight sequential steps. The first ones are primarily related to process the satellite data in order to be ready to interpret the values of each area. These are the SAR image rectification and calibration, image co-registration to the reference data and the calculation of backscattering coefficients for different forest stem volume classes. The following steps are the core of the method, where the first one is the forest compensation, after that the linear interpolation phase of SCA estimation and finally, the weather station assimilation procedure.

Forest compensation procedure reduces the effect, and therefore the error, of the forest canopy on the SCA estimates. It minimises the variation in the backscattering coefficients introduced by the forest. The main calculation inside this algorithm is based on the boreal forest semi-empirical backscattering model developed also at TKK [2]. In summary, it generates an estimate of the contribution made by backscattering due to the forest canopy, which then is subtracted from the total observed backscattering value resulting in the forest compensated value. The next equation describes the variables affecting this coefficient:

$$\sigma^o(V,a,\theta,\sigma^o_{surf}) = \sigma^o_{surf} \cdot \exp\left(\frac{p_1 \cdot a \cdot V}{\cos\theta}\right) + p_2 \cdot a \cdot \cos\theta \cdot \left[1 - \exp\left(\frac{p_1 \cdot a \cdot V}{\cos\theta}\right)\right] \equiv \sigma^o_{surf} \cdot t(V,a,\theta)^2 + \sigma^o_{can} \cdot t(V,a,\theta) \quad (2)$$

Both terms are primarily affected by V (forest stem volume [m^3/ha]), a (used to define the conditions of forest canopy), and θ (the angle of incidence). The first term of (2) defines the backscattering contribution from the ground or snow layer σ^o_{surf} and the two-way transmittivity through the forest canopy (t^2). The second one describes the forest canopy backscattering contribution, σ^o_{can}.

Once the effect of forest canopy is calculated, it is subtracted independently for each drainage basin, and the compensated backscattering values are used in the linear interpolation stage of the SCA estimation. This phase is based on the assumption that the observed surface backscattering is a linear combination of backscattering from the area covered by snow and the area of snow-free ground. Therefore, this algorithm needs to know these two backscattering values before being able to perform the estimation. It is done using two

reference images, one with the features at the beginning of the melting process and the other acquired at the end of the melting process. The SCA result is a percentage indicating the fraction of ground covered by snow for each area, and it is obtained by:

$$SCA = 100\% \cdot \frac{\sigma^{\circ}_{surf} - \sigma^{\circ}_{ground,ref}}{\sigma^{\circ}_{snow,ref} - \sigma^{\circ}_{ground,ref}} \qquad (3)$$

The σ^{o}_{surf} is the measured value of the image under analysis after the forest compensation, $\sigma^{o}_{ground,\ ref}$ is the reference backscattering coefficient from the snow-free ground and $\sigma^{o}_{snow,\ ref}$ is the coefficient from the wet snow-covered ground at the beginning of the melting period.

The last stage of the method is the weather station assimilation procedure (WSA). The SCA estimation works by looking at the difference between the coefficients returned from wet snow surfaces and the bare ground, which is usually wet, being the situation during the melting process. After the snow melt season ends, the ground dries decreasing the backscattering levels [10]. As a consequence, bare ground situations can be falsely categorized as snow-covered. The objective of this method is to use the ground-based weather station data for determining whether the snow-melt season has actually finished, avoiding the formation of false estimates.

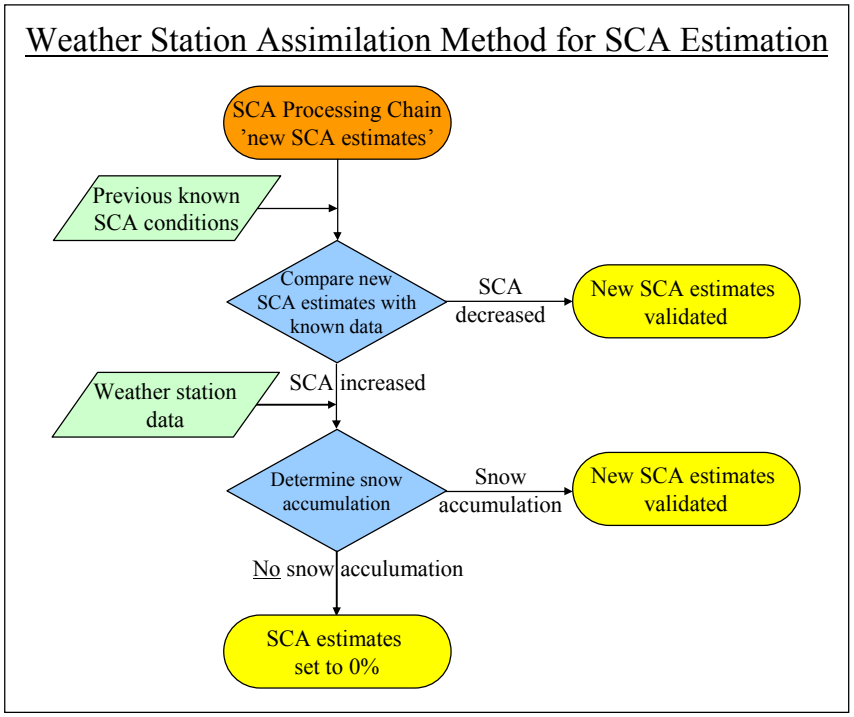

Figure 5, the weather station assimilation procedure

The first step in the algorithm is to check if the new SCA estimate for each drainage basin presents an increase with respect to the previously analysed data. In these cases, the weather

station data is analysed. If the weather station data shows negligible snow accumulation and the SCA estimate shows increased values, the SAR-based SCA estimates are corrected to indicate snow free conditions. Otherwise, if the weather station data confirms the snow accumulation between either images or the SCA estimate has decreased, the new estimates are validated.

The correction of the SCA estimation by the weather station assimilation method for the image acquired on *12 May 2006* where the dominating situation was bare ground is shown in Figure 6:

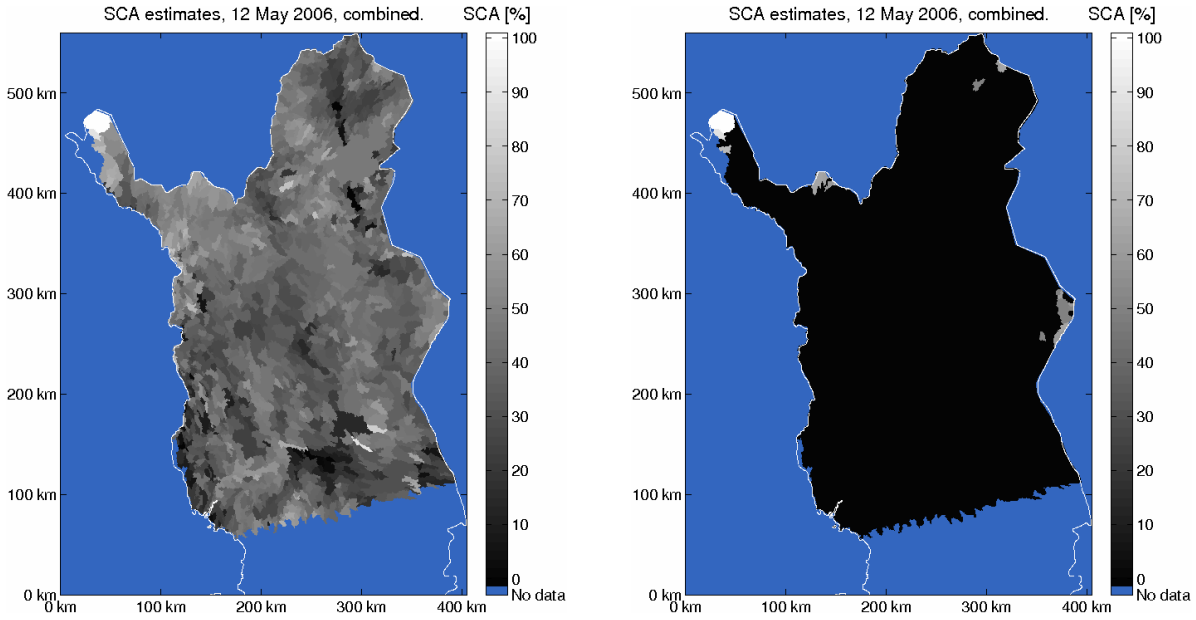

Figure 6, Comparison between the SCA carried out without WSA at left and using it at right

This example demonstrates the great amount of erroneous pixels in the estimate carried out without the WSA presented on the left. Typically, this method improves the accuracy at end of the melting season when the backscattering values undergo conditions not completely related to the snow conditions.

2.6 Snow-Covered Area Estimation with MODIS-Data

The Snow-Covered Area (SCA) estimation based on remote sensing data has been widely studied. The estimation using optical data from satellites have achieved great accuracy, and therefore, the Finnish Environment Institute has included the MODIS based method in the forecast of the snow melting season in Finland [10]. The *SCAmod* estimates have also been assimilated to the Finnish national hydrological modelling and forecasting system since 2003, showing a substantial improvement in accuracy of the predictions.

Optical sensors are able to distinguish between snow-covered and snow-free ground because of the high reflectance of snow in certain wavelengths compared with other natural targets [10]. However, the main problem in Finland is the larger areas dominated by forests. These areas are constantly changing and as a consequence, require a feasible and reliable remote sensing method. In this respect, this method combines two different procedures for estimating the SCA for both forested and non-forested areas.

The method for SCA estimation is based on the high reflectance of snow compared with other natural targets. The equation below defines this calculation:

$$SCA = \frac{\frac{1}{t_\lambda^{\,2}} \cdot \rho_{\lambda,obs}(SCA) + \left(1 - \frac{1}{t_\lambda^{\,2}}\right) \cdot \rho_{\lambda,forest} - \rho_{\lambda,ground}}{\rho_{\lambda,snow} - \rho_{\lambda,ground}} \qquad (4)$$

Where $\rho_{\lambda,obs}$(SCA) is the observed value depending on the SCA, the $\rho_{\lambda,forest}$, $\rho_{\lambda,ground}$ *and* $\rho_{\lambda,snow}$ are the generally applicable reflectances for dense coniferous forest canopies, snow-free ground and wet snow at the wavelength λ, respectively. The calculations include a measure for effective transmissivity t_λ defined in the equation:

$$t_\lambda^{\,2} = \frac{\rho_{\lambda,obs}(SCA = 1) - \rho_{\lambda,forest}}{\rho_{\lambda,drysnow} - \rho_{\lambda,forest}} \qquad (5)$$

The SCAmod method also implements the Normalized Difference Vegetation Index (NDVI) rule which reduces the overestimations produced by the appearance of seasonal green vegetation at the end of the melting season. Typically, NDVI increases suddenly at the beginning of ground season. When it exceeds the NDVI threshold value, the SCA estimate is 0% [10].

2.7 Snow-Covered Area estimated according to the proposed Algorithm of Thomas Nagler and Helmut Rott

2.7.1 Introduction

This method was developed for mapping wet snow in mountainous areas and was tested in the Eastern Alps of Austria. The data was acquired via a European Remote Sensing satellite (ERS 1/2) and Radarsat synthetic aperture radar (SAR). The drainage basin under study was Tuxbach where the dominating surface class was low vegetation made up of alpine meadows and dwarf shrubs located at higher elevations, as well as cultivated meadows in the valleys. There were also dispersed areas with/made up of bare soil and rocks, a glaciated area (over 3%) and Coniferous forests (approximately 11%).

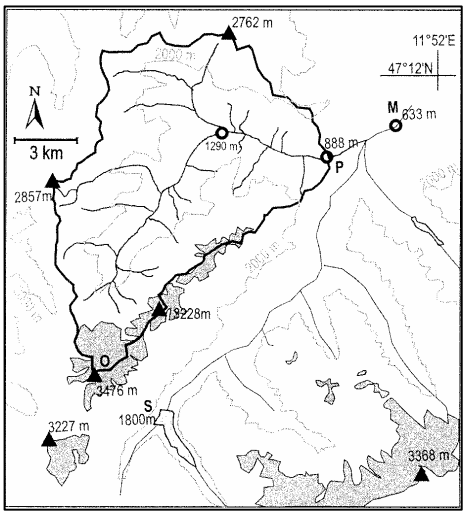

Figure 7, Drainage Basin Tuxbach

The algorithm is based on the backscattering properties of snow-free and snow-covered alpine surfaces. Additionally, the alpine region presents a great difficulty with highly varying topography. The variation in this terrain implies a high range of different incidence angles and consequently, different backscattering coefficients for the same kind of surface. In order to improve the accuracy of the algorithm, a digital elevation model (DEM) with 25-m grid spacing was generated to calculate the local incidence angle for each pixel before averaging the backscattering of the amount of each angle step pixels. It was noted that the averaged backscattering decreases when the incidence angle increases for all the three main situations, whether dry snow, wet snow or bare ground. Furthermore, the variation in the data during the whole year was measured. As a result of the state of the ground (free-snow, wet, refrozen snow, dry snow or wet snow), an important decrease in the backscattering value was observed during the melting season for the three kinds of area analysed. In addition, the influence of the

roughness in the backscattering of wet snow was demonstrated through a test carried out in the ski tracks in the glacier plateau of Kesselwandferner.

2.7.2 Wet Snow Mapping Algorithm

An essential objective of the snow mapping algorithm is to eliminate the topographical effects on the data received to improve the accuracy of the estimations. The main basis is the comparison between the lowest backscattering coefficients of melting snow and the reference images. Therefore, these images are needed in the same imaging geometry in one of the two scenarios: ground which is either free of snow or completely covered with dry snow.

The complete process is divided into three principal parts, where each is dependent on the previous step. The first includes coregistration, calibration, speckle reduction, and geocoding. The resulting files (both ascending and descending images) are geocoded ratio images of the snow correlated with the reference image, which is necessary to generate the final estimate. Therefore, the core of the estimate is within the second step, and it works according to the following pixel by pixel discrimination rules:

1. ***if (L = True or S = True or $\theta i < 17°$ or $\theta i > 78°$)***

   Snow mapping is not possible

2. ***else if ($\sigma°_{ws} / \sigma°_{ref} < TR$)*** *wet snow*

3. ***else*** *snow free or dry snow*

The first rule eliminates all pixels affected by layover, radar shadow, or inappropriate local incidence angles, looking for valid pixels in both node images (ascending and descending) and selecting the best one. Once there is valid data, the algorithm compares for each pixel the value of the ratio with a threshold level (-3dB being the most appropriate) and decides “1” if is lower or “0” if is higher.

The final snow-covered area estimate is realized by averaging the total pixels for the analysed area. The last part applies postprocessing rules to split up the amount of pixels referring to melting areas of the remaining pixels. It is useful because both dry snow in the high elevations and free snow agricultural areas in the valleys cause important changes in the backscattering data not related to snow melt. Algorithm is presented in [1].

2.8 Accuracy Assessments

The main objective of the project is to determine the accuracy of the snow-covered area estimates by comparing them to the estimates based on optical data that are expected to be more accurate. Therefore, the statistical tools used during this evaluation are based on quantifying the amount by which this estimator differs from the true value, in this case the optical estimates. The primary calculation was the root mean squared error or RMSE.

The Root Mean Squared measured the average magnitude of the error. Essentially, it works averaging the difference between the forecast and corresponding values observed over the sample. Finally, the square root of the average is taken. Since the errors are squared before they are averaged, the RMSE gives greater weight to large errors, represented in the following equation:

$$RMSE = \sqrt{\frac{\sum_{i=1}^{n}(x_i - y_i)^2}{n}} \qquad (6)$$

Other statistical calculations were also used inside this study but with less importance for the analysis procedure; the mean absolute error, the correlation coefficient and the bias evaluations:

The Mean Absolute Error, as the name indicates, is a weighted average of the absolute errors which are the difference between the prediction and the true value. Equation (7) below describes this calculation:

$$MAE = \frac{\sum_{i=1}^{n}|x_i - y_i|}{n} \qquad (7)$$

The Correlation Coefficient is typically used as an indicator of the relationship between two variables. This value changes between 0, and 1, being 1 if both have the same value. The next equation describes this calculation:

$$r = \frac{n \cdot \sum x_i \cdot y_i - \sum x_i \sum y_i}{\left[n \cdot \sum x_i^{\,2} - \left(\sum x_i\right)^2\right]^{1/2}\left[n \cdot \sum y_i^{\,2} - \left(\sum y_i\right)^2\right]^{1/2}} \qquad (8)$$

The Bias is described in the next equation:

$$bias = \frac{\sum_{i=1}^{n} x_i - y}{n} \qquad (9)$$

2.9 Adapting the Nagler & Rott Algorithm to the TKK Automatic Processing Chain

The main objective of this study is to evaluate the snow-covered area (SCA) estimation developed by Nagler and Rott on boreal forest zone. The algorithm is merged to the automatic image processing software created by the Laboratory of Space Technology at the Helsinki University of Technology (TKK) for data analyses. This new estimation method requires the backscattering data for each pixel in order to calculate the SCA without averaging the amount of backscattering coefficients. Therefore, it is incompatible with the actual forest compensation step, which has been removed. The SCA_estimation and Sigma0_calculation steps have also been removed and now are included into the *SCA_ nagler* script.

The new process chain

The correct operation of the process chain was evaluated and proven using this alternative method. It implies the most basic level estimation, without taking into account either the stem volume information or the incidence angle information. Furthermore, the chain generates two outputs, one map in TIFF-format and a matrix where are stored the SCA estimates, but without distinguishing between open and forested areas.

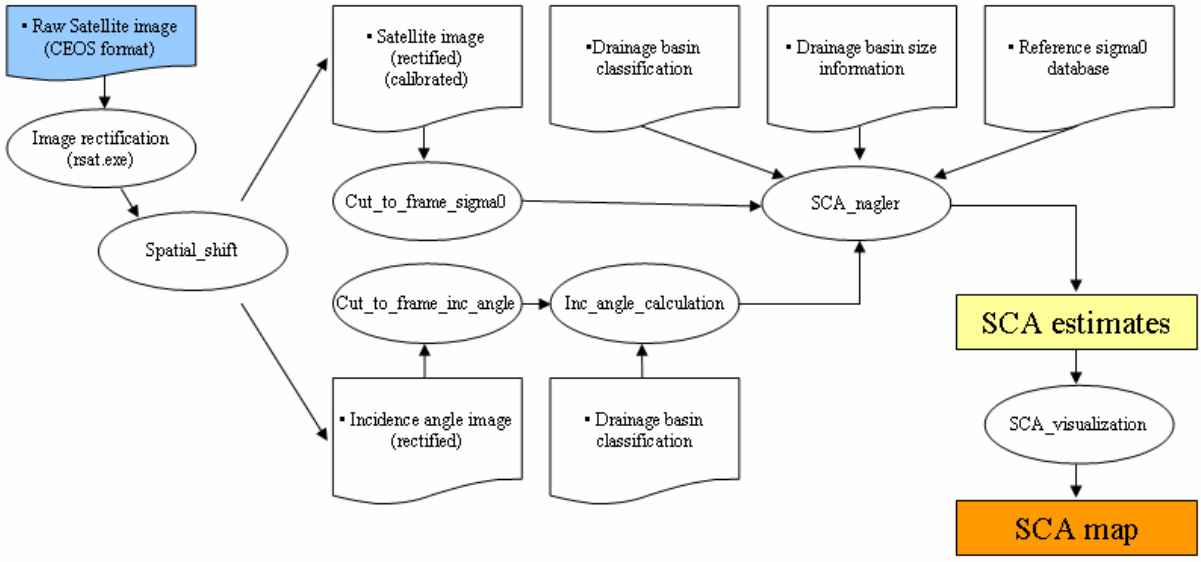

Figure 8, the processing chain for SCA estimation

The complete description of the original TKK process can be found in the document [4], the SCA_nagler script is presented in the appendix I.

3 Test Site and Satellite Data

Following on from the latest studies carried out using the TKK method and being able to compare the accuracy of the TKK and Nagler & Rott methods, the Satellite Data used in this work is the same that used in the most recent studies at TKK [2], [8] (acquired between 2004 and 2006). The test site is located in northern Finland bounded by the Finnish state borders and spans between 65º and 70º, northern latitude. Figure 9 shows the covered area for a typical Radarsat scanSAR wide image:

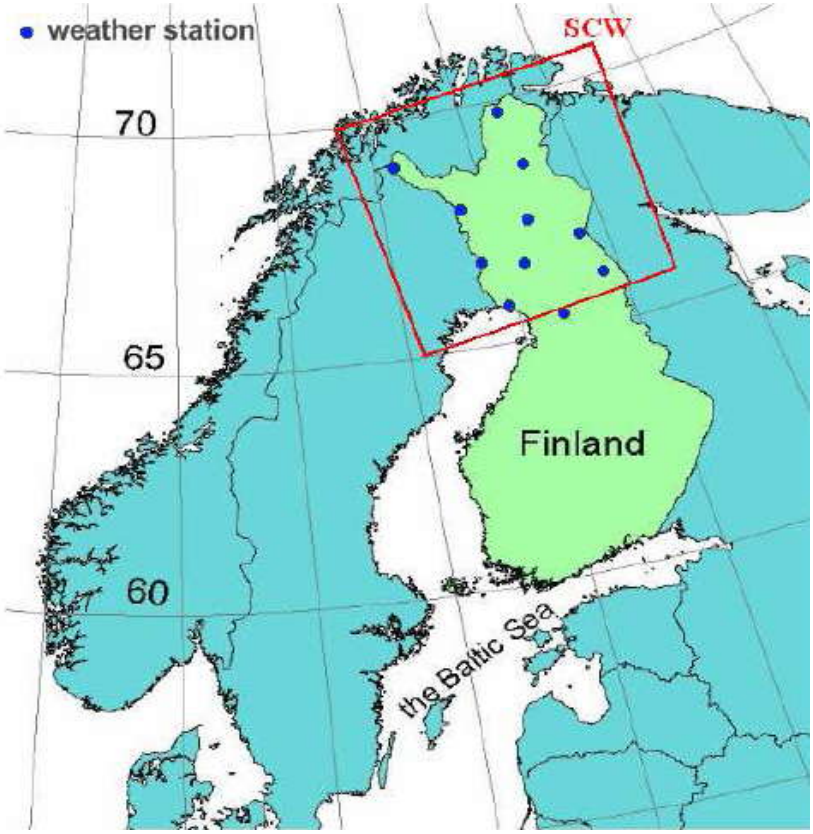

Figure 9, the coverage shown for Radarsat

This region presents a landscape with modest topography and is largely dominated by typical northern boreal forests as sparse coniferous forest (over 43%), with some open areas (approximately 50%), which usually are bogs/marshland. The remaining area is water pixels which are not used in the SCA estimation. The covered area is divided into 2037 smaller areas each corresponding to a drainage basin, the drainage basin categorization is based on the Finish Watershed Simulation and Forecasting System (WSFS) [23]. The drainage basin classification and the reference data have a 100 m x 100 m spatial resolution while the average size of each basin is approximately 74.9 km^2. The SCA estimates were carried out independently for each computational unit taking into account the information of the analysed area. Furthermore, it also allowed testing the behaviour of the data in each kind of area; forested, open and combined.

3.1 The Satellite SAR Data Set

The satellite SAR data was acquired during the snow melt seasons of 2004, 2005 and 2006, all from the ascending node and using the imaging mode ScanSAR Wide A (SCW), which provides an operationally well usable 500km swath width employing HH-polarization. The total amount of Radarsat SAR intensity images for the analysis was 14. Each image was rectified and processed using the orbital parameters and calibration information given by the satellite data provider: Kongsberg Satellite Service AS. The rectification by orbital parameters was evaluated by measuring the locations of known ground control points. The small residual errors were corrected by manually co-registering the images and the reference data. The SAR images, the acquisition dates, the averaged incidence angles, and the stages of the snow melt season are described in Table 1.

Table 1, Radarsat SCW Satellite Dataset

Date	Center inc.angle	Progress of snow melt season
18 April 2004	30.8°	Beginning of melt season
28 April 2004	36.2°	Middle of melt season
5 May 2004	33.9°	Middle of melt season
12 May 2004	31.7°	Middle of melt season
26 May 2004	**25.7°**	**End of melt season**
30 March 2005	**36.1°**	**No snow melt (dry snow)**
30 April 2005	33.6°	Beginning of melt season
7 May 2005	30.9°	Beginning of melt season
14 May 2005	28.1°	Middle of melt season
31 May 2005	**30.9°**	**End of melt season**
2 May 2006	30.9°	Beginning of melt season
5 May 2006	38.5°	Middle of melt season
9 May 2006	28.1°	End of melt season
12 May 2006	**36.1°**	**End of melt season**

The influence of the incidence angle on the estimation has been assessed [3] and becomes more important if there are larger differences between the incidence angle of the reference image and the analysed image. However; the maximum deviation in this data set was approximately 10.4º and was not expected to be significant.

The image candidates for reference image (marked in bold) are labelled as *"End of melt season"*. Typically these images correspond to situations close to 0% SCA or bare ground, therefore, their features are appropriated to use in the discrimination process. Furthermore, the image labelled as *"No snow melt (dry snow)"* was also expected to be useful in this process because the main features are similar. The SCA estimates were determined for the images acquired during the snow-melt season but at different stages of the process and, consequently,

with different SCA values, excluding those marked in grey because there existed no optical data available to test their accuracy.

3.2 Optical Remote Sensing Data

The assessment of the accuracy was carried out by comparing the estimates derived from Radarsat data to the SCA estimates acquired by optical satellite data. The snow melting in Finland has been operatively monitored with SCAmod in Finnish Environment Institute (SYKE) since year 2001 covering 5845 basins. It was designed to best perform for boreal forest areas and is feasible in operational use (Section 2.6). The optical SCA method has been shown to have good accuracy and the validations with in situ data indicated around 10% RMSE value [2], [9].

Table 2, the reference satellite dataset (TERRA/MODIS)

Date	Reference to	Separation	Coverage
26 April 2004	28. April	2 days	21 %
27 April 2004	28. April	1 days	66 %
28 April 2004	28. April	0 days	83 %
3 May 2004	5. May	2 days	6 %
6 May 2004	5. May	1 days	92 %
7 May 2004	5. May	2 days	55 %
2 May 2005	30. April	2 days	23 %
12 May 2005	14. May	2 days	5 %
14 May 2005	14. May	0 days	63 %
16 May 2005	14. May	2 days	35 %
1 May 2006	2. May	1 days	97 %
2 May 2006	2. May	0 days	92 %
3 May 2006	2. May / 5. May	1 / 2 days	45 %
4 May 2006	2. May / 5. May	2 / 1 days	30 %
5 May 2006	5. May	0 days	82 %
6 May 2006	5. May	1 days	90 %
7 May 2006	5. May / 9. May	2 / 2 days	90 %
8 May 2006	9. May	1 days	73 %
9 May 2006	9. May	0 days	25 %
10 May 2006	9. May / 12. May	1 / 2 days	17 %

The current data used in this study was acquired by Terra/MODIS during the years *2004* to *2006* [2], [9]. Since the optical data is not always available because of the weather and illumination conditions, sometimes it is not possible to have suitable reference data to compare with the radar based SCA estimates. However, it is useful to utilize all the data that is acquired with a small temporal difference. Coverage of almost the whole image can be achieved by combining optical data from several days. In this study all the images with a

maximum deviation off 2 days have been used, all these images are listed in the table 2. The wide variation on the coverage can be seen due to the bad visibility conditions.

3.3 Weather Station Ground Truth Data

There are around fifty weather stations along Finland where each one conducts daily measurements and registers the information about the temperatures, precipitation, cloud, and wind conditions. Eleven of these stations (marked on the figure 9) are inside the area of Northern Finland, under study, providing extra information used on the analysis of the variables affecting the accuracy on the threshold level selection. Moreover, this data is totally necessary when applying the Weather Station Assimilation procedure of the TKK SCA method.

3.4 Drainage Basin and Stem Volume Data

The Watershed Simulation and Forecasting System is widely used in Finland for real time hydrological simulation and forecasting. WSFS covers the land area of Finland including cross-boundary watersheds. The main distribution is based on a 60 – 100 km^2 sub-basins division with the total amount 5500 basins. In this study the same drainage basin classification and location information has been used. In northern Finland there is 2037 drainage basins.

The land-use classification data have been produced by the National Land Survey of Finland using the National Forest Inventory data [23]. This data has a 25 m x 25 m resolution and it is based on cartographic data, ground truth sampling and Landsat TM imagery. The main information used in this study is the variation of the stem volume in order to discriminate between forested areas and open areas according to the classification of these volume classes; 0-50, 50-100, 100-150, 150-200, and over 200 m^3/ha.

4 Evaluation of the accuracy of the Nagler & Rott SCA estimation algorithm in Northern Finland

The purpose of this chapter is to show the accuracy of the Nagler & Rott SCA method developed for a specific area when applied to another geographical area with completely different topography: importing a system from alpine areas to the boreal forest of Northern Finland. This algorithm estimates the SCA where the evaluation is based on the backscattering levels measured by Radarsat.

4.1 Analysis of the SAR Data Set

The melting process of snow can be monitored using radar data by looking at the variations on the backscattering contributions. In fact, the backscattering level experiences a progressive reduction whereas the snow-melt season makes progress. The backscattering level of wet snow is typically affected by the air-snow contribution variables; the snow liquid water content and the roughness of the surface being the most important. These backscattering levels could reach the same value as the dry or the bare ground situation when the surface has a high roughness with also low snow liquid water content (snwc). In contrast, dry snow and also bare ground are widely dominated by the snow-ground contribution. In that case the incidence angle has an important influence being approximately -2dB with an increase of 10 degrees [3]. In addition, the higher value in the bare ground situation is measured just at the end of the melt season when the ground is wet and becomes lower as the ground dries out. The data in the Table 3 has been organized by the backscattering level:

*Table 3, Averaged temperature, rain and backscattering for each image organized by the backscattering value from the lowest to the greatest. Marked in grey are the images without optical data to compare and in **bold text** the reference images.*

	Averaged Values				
Image (inc.angle)	**Temperature (°C)**	**5 prior days Temperature (°C)**	**Rain (litres)**	**5 prior days Rain (litres)**	**Backscattering**
30 April 2005 (33.6°)	1.0	2.9	0.0	0.0	-12.027
18 April 2004(30.8°)	---------- No weather station data available ----------				-11.791
28 April 2004 (36.2°)	4.0	0.5	0.0	0.0	-11.299
07 May 2005 (30.9°)	0.2	-0.2	4.7	16.0	-10.692
***30 March 2005** (30.8°)*	**0.0**	**-2.1**	**0.0**	**11.5**	**-10.407**
14 May 2005 (28.1°)	5.6	3.6	0.7	17.3	-10.298
***12 May 2006** (36.1°)*	**7.0**	**8.5**	**1.5**	**3.0**	**-9.839**
12 May 2004 (31.7°)	13.8	11.9	0,3	1.7	-9.826
02 May 2006 (30.9°)	7.3	6.2	0.0	1.6	-9.655
05 May 2004 (33.9°)	10.1	6.1	1.2	2.1	-9.639
05 May 2006 (38.5°)	8.0	7.4	0.0	0.0	-9.524
***31 May 2005** (30.9°)*	**4.0**	**6.2**	**0.3**	**14.8**	**-9.171**
09 May 2006 (28.1°)	10.8	11.2	0.0	0.0	-8.901
***26 May 2004** (25.7°)*	**4.2**	**4.8**	**1.1**	**13.7**	**-8.871**

As it was expected, most of the data followed a chronological organization directly related to the averaged backscattering level. The first available data acquired during 2004 presented some strange behaviour. The image from 12 *May 2004* had a lower averaged backscattering value than the image from *5 May 2004*. The difference is relatively insignificant (0.2 dB) if it is not taken into account that there are 7 days between both, with high temperatures. This could be because of the contribution of the south areas where the bare ground was more dried than in the image of *5 May*. The data from second year (2005) presented an expected behaviour and the change in backscattering followed a chronological order. Finally, the last year data was almost as expected, but the image acquired from the 12 May 2006 had the lower value which was not expected. It can be explained looking at the incidence angle during the measurements. In that case, the measured value was almost 5 degrees higher than the image acquired on *2 May 2006* and *9 May 2006*. On the other hand, it was lower than the incidence angle on the image of *5 May 2006* but the backscattering value of this one was greater. It could be explained because the image of *12 May 2006* was almost totally dominated by a bare ground situation and as a consequence, the backscattering value was largely affected by the incidence angle, but the image of *5 May 2006* was not, since it had many areas with wet snow.

4.2 Influence of the Reference Image Selection and Threshold level on SCA estimation Accuracy

In the study the Reference Images were necessary in order to estimate the snow covered area. These images were also part of the accuracy analysis and they determine the backscattering levels for SCA estimation. To choose the most suitable ones was one of the most important objectives. Four images were used, three as the reference for the bare ground and one for the dry snow situation. Bare ground and dry snow images, were expected to be useful in this analysis because both have high backscattering levels. Naturally, the variations in the data cause significant differences between the averaged backscattering levels of each image and as a result, the optimal threshold level changes for each one. The accuracy evaluation was done for each drainage basin and also for each kind of area (open, forested and combined) by comparing the radar derived estimates to the data acquired from optical satellite data (MODIS). It was considered that forested areas were at least covered 75% by trees whereas the open areas were covered less than 25% by trees.

4.2.1 Results using bare ground SAR images as reference data

The starting point was assessing the accuracy using the threshold level of -3dB proposed in the implementation of the Thomas Nagler & Helmut Rott Snow Mapping Algorithm [1]. The results of RMSE calculations for open, forested and combined areas are shown in Table 4.

Table 4, accuracy results for SCA estimation with each reference image using -3dB threshold level

Reference Image	**26 May 2004**			**31 May 2005**			**12 May 2006**		
Area	Combined	Open	Forested	Combined	Open	Forested	Combined	Open	Forested
RMSE	0.307	0.300	0.387	0.344	0.315	0.389	0.388	0.370	0.435
Mena abs. error	0.239	0.238	0.295	0.269	0.247	0.293	0.306	0.291	0.330
Bias	-0.212	-0.217	-0.277	-0.251	-0.225	-0.270	-0.299	-0.281	-0.319
Correlation coefficient	0.822	0.867	0.762	0.816	0.843	0.711	0.789	0.824	0.714
Samples	9148	506	525	9790	541	556	9835	540	557

Unfortunately, the results obtained were very poor when compared to the outcomes of the TKK method [2], [8]; even the best ones achieved using the reference image of 2004. Hence this threshold level is not suitable to estimate the SCA on boreal forest zone. However, it was

demonstrated by R. Magagi and M. Bernier [3] in their measurements that the level between snow and wet backscattering could have approximately a difference of -1dB. In this respect, they explained that the adaptation of one method to another surface is not easy and as consequence, the optimal threshold level changes. Moreover, the incidence angle has an effect reducing the backscattering level whereas it increases. This could perhaps also explain the poor result because the topography was different when compared with the Nagler and Rott area analysed, and as a consequence, the incidence angles were smaller in northern Finland.

It was necessary then to start looking for the best threshold level for this new topographical area dominated by boreal forest. The first step was to calculate the averaged backscattering value for each area and image analysed, excluding those images used as reference image. This value is important since, as shown in the summary, the backscattering coefficient increases while the melt season progresses. In this context, the reference images must have a low level of backscattering in order to be useful in the discrimination process. The averaged backscattering levels for the analysed data set are shown in Table 5:

Table 5, averaged backscattering for all images under study

Averaged Backscattering (dB)				
	Combined	Open areas	Forested areas	
Image				Incidence Angle
18 04 2004	-11.791	-12.768	-10.792	30.8°
28 04 2004	-11.298	-12.051	-10.613	36.2°
05 05 2004	-9.638	-10.035	-9.178	33.9°
12 05 2004	-9.825	-9.972	-9.643	31.7°
30 04 2005	-12.026	-12.797	-11.240	33.6°
07 05 2005	-10.692	-11.482	-9.889	30.9°
14 05 2005	-10.298	-11.042	-9.533	28.1°
02 05 2006	-9.655	-10.137	-9.122	30.9°
05 05 2006	-9.523	-9.914	-9.082	38.5°
09 05 2006	-8.901	-9.022	-8.756	28.1°
Averaged value	-10.392	-10.975	-9.789	
Minimum value	-12.026	-12.797	-11.240	
Maximum value	-8.901	-9.022	-8.756	

It is interesting to note the approximate 3dB difference between the higher and the lower averaged level because it shows the variation of the SCA between April and May. In fact the lower value limits the minimum averaged value for the reference images being approximately -9dB. In addition, the most important value from this investigation corresponds to the

averaged value of all the images. This overall average backscattering level could indicate the approximate threshold level suitable for SCA estimation.
The following step in this process was to search for the best accuracy by sweeping a large range of threshold levels, starting at -2.5dB to -0.5dB with a resolution of 0.2 dB for each step. In the next pages the results are shown which take into account all the analysed images and compare them with the principal features of each reference image.

12 May 2006 as reference image

The first SAR image studied as a reference image was acquired on the 12th May 2006 when there were bare ground conditions. The averaged backscattering is shown in the table below and it is also compared to the average, the minimum and the maximum value of all the images under study (Table 5).

Table 6, averaged backscattering for the image 12th May 2006

Averaged Backscattering (dB)			
Reference Image	**12 May 2006**		
	Combined	Open	Forested
Averaged Value	-9.839	-10.112	-9.522
Averaged difference	**-0.55**	**-0.85**	**-0.27**
Minimum difference	0.93	1.09	0.76
Maximum difference	-2.18	-2.68	-1.71

The results obtained predict an inaccurate estimate, at least for some images, because the average value is lower than the calculated value for some of the images studied. Furthermore, the difference from the minimum value is close to 1dB positive, which means that the estimate for this image is rarely accurate. The averaged difference is also very small which implies a lower threshold level selection in order to make correct estimates. Figure 10 showed the experimental searching of the threshold level for the complete set of images, representing more than 10 simulations and assessments for each area:

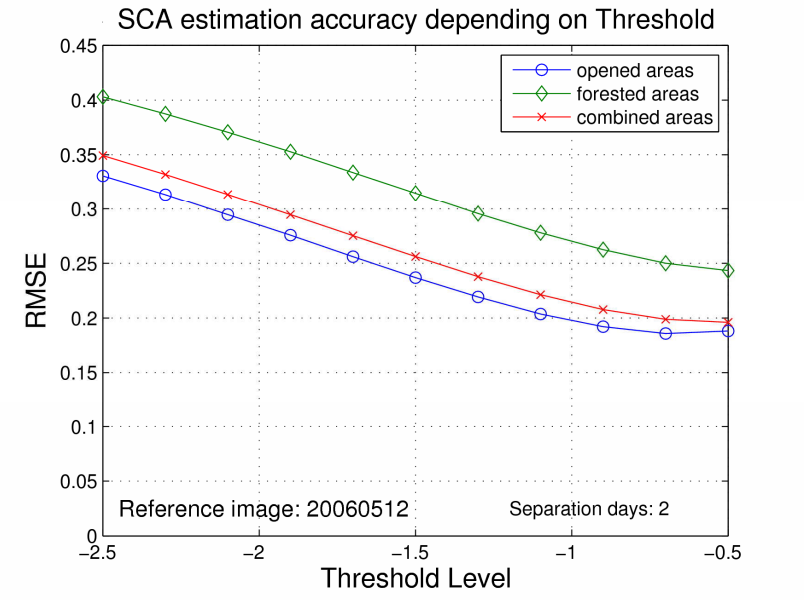

Figure 10, RMSE variation sweeping the Threshold level between -2.5dB and -0.5dB for each area with 0.2 dB of resolution. (557 samples forested areas, 540 samples open areas, and 9835 samples combined areas).

It is noted in Figure 10, how the minimum RMSE value for each curve is closely related to the averaged difference value (text coloured red in Table 6) as threshold level for all the three kinds of areas. In this case, it means a very low threshold level which is too small to produce accurate estimates. This behaviour is caused by the lower backscattering levels of the reference image as explained before.

31 May 2005 as reference image

The second SAR image studied as a reference image was acquired on the 31th May 2005 when there were bare ground conditions. The averaged backscattering coefficients are shown in Table 7 which also compares to the average, the minimum and the maximum value of all the images under study (Table 5).

Table 7, averaged backscattering for the image 31 of May of 2005

Averaged Backscattering (dB)			
Reference Image	**31 May 2005**		
	Combined	Open	Forested
Averaged Value	-9.171	-9.477	-8.819
Averaged difference	**-1.22**	**-1.49**	**-0.97**
Minimum difference	0.26	0.45	0.06
Maximum difference	-2.85	-3.32	-2.42

In this case, the difference with the biggest value of the analysed images is lower and close to zero because the averaged value of this reference image is approximately -9dB. Moreover, the averaged difference is greater in this case and near to -1dB, which implies a threshold level value within the range studied by R. Magagi and M. Bernier [3]. Figure 11 shows the experimental searching of threshold for this level, representing there more than 10 simulations and assessments for each investigated area.

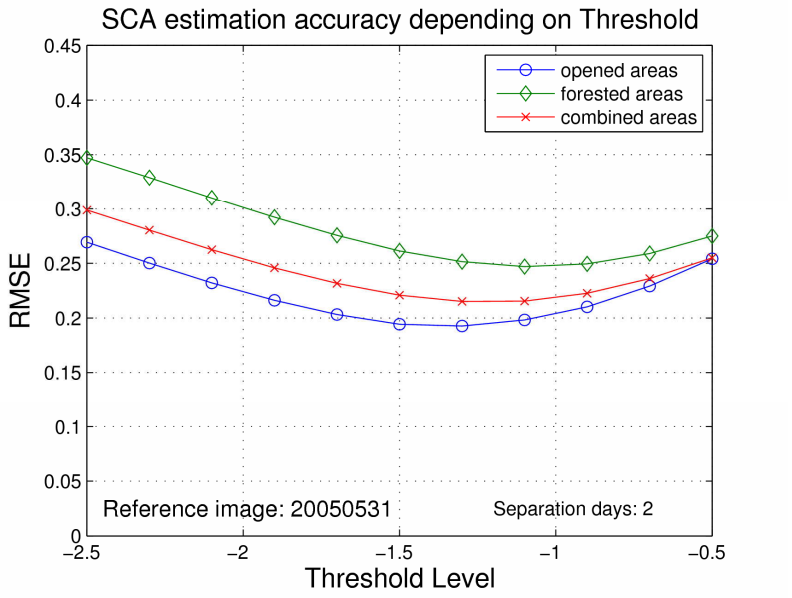

Figure 11, RMSE variation sweeping the Threshold level between -2.5dB and -0.5dB for each area with 0.2 dB of resolution. (556 samples forested areas, 541 samples open areas, and 9790 samples combined areas).

It is seen in Figure 11 how the minimum RMSE value for each curve is closely related to the averaged difference value (text coloured red in the table 7) as the threshold level for all the different areas.

26 May 2004 as reference image

The final SAR image studied was acquired on the 26th May 2004 with bare ground conditions. The averaged backscattering is shown in Table 8 which also compares the data to the average, the minimum and the maximum value of all the images under study (Table 5).

Table 8, averaged backscattering for the image 26 of May of 2004

Averaged Backscattering (dB)			
Reference Image	**26 May 2004**		
	Combined	Open	Forested
Averaged Value	-8.871	-8.928	-8.799
Averaged difference	**-1.52**	**-2.04**	**-1**
Minimum difference	-0.03	-0.09	0.04
Maximum difference	-3.15	-3.86	-2.44

As seen in Table 8, the averaged value in this case is greater than the maximum of the images under study (approximately -9dB; Table 5) and it is also reflected in the minimum difference value. Consequently, it is expected to be useful as a reference image in the analysis. Additionally, the averaged difference for SCA estimation is inside the range proposed by R. Magagi and M. Bernier [3]. Figure 12 shows the experimental searching of the threshold level, representing there more than10 simulations and assessments for each area:

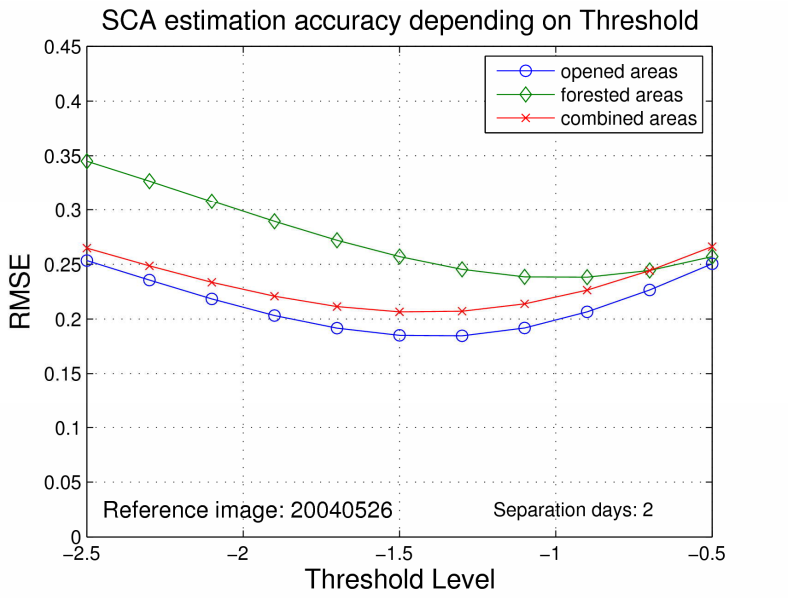

Figure 12, RMSE variation when the Threshold level is swept between -2.5dB and -0.5dB for each area with 0.2 dB of resolution. (525 samples forested areas, 506 samples open areas, and 9148 samples combined areas).

It can be seen in Figure 12 how the minimum RMSE value for each curve is closely related to the averaged difference value (red in the table 8) as the threshold level for each of the three different areas.

The main conclusion drawn up to this point was that each reference image has a different useful threshold level which is directly proportional to the average backscattering level of the snow-melt images. As a consequence the following analyses were done in the range where the optimal threshold level for each area and reference image was expected to be found. The resolution was increased to 0.05 dB in order to obtain more accurate discrimination for these analyses.

12 May 2006 as reference image

Figure 13 below shows the detailed searching of threshold level using *12 May 2006* as a reference image, representing 13 simulations and assessments for each area.

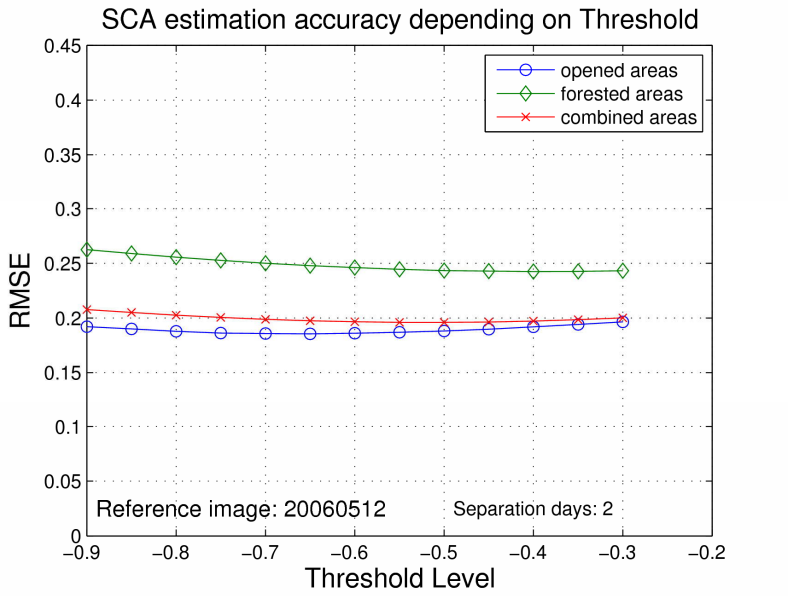

Figure 13, RMSE evolution when the Threshold level is swept between -0.9dB and -0.3dB for each area with 0.05 dB of resolution (557 samples forested areas, 540 samples open areas, 9835 samples combined areas).

The variation inside the detailed range is almost unnoticeable and differs very little from the results obtained with a 0 dB threshold level. The table below shows the minimum acquired RMSE related to the optimal thresholds.

Table 9, optimal threshold levels with 12 May 2006 image as reference

Area	Optimal Threshold	RMSE
Open	***-0.65 dB***	0.185
Forested	***-0.4 dB***	0.242
Combined	***-0.5 dB***	0.196

These results are explained by looking at the variation of the features between all the tested images. In particular, there are some images with higher averaged backscattering values than this reference image. These optimal levels, generally speaking, are the best ones to use when the complete data set is processed, however, it is not possible to extrapolate them for each independent image. Furthermore, these thresholds are too minute to be able to discriminate

between both surfaces. In conclusion, the *12 May 2006* image is not useful as a reference image for SCA estimation.

31 May 2005 as reference image

Figure 14 below shows the detailed searching of threshold level using *31 May 2005* as a reference image, representing 13 simulations and assessments for each area.

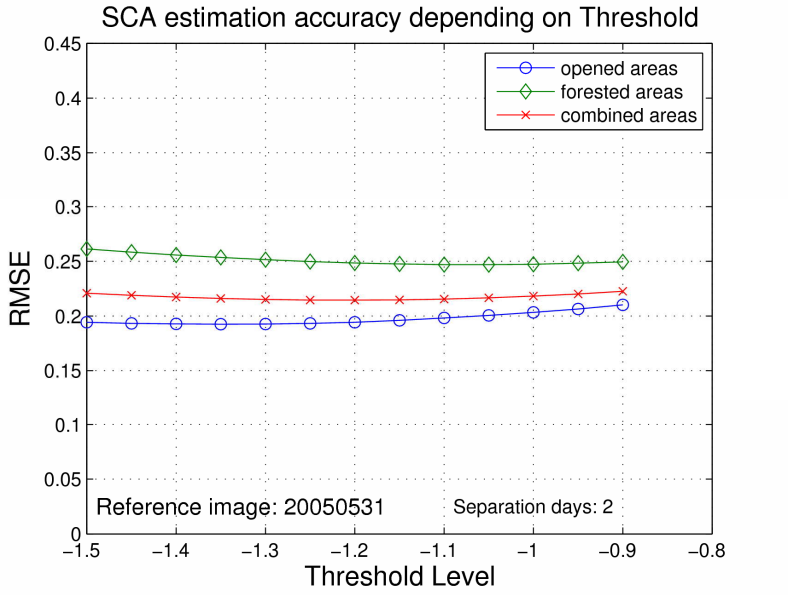

Figure 14, RMSE evolution when the Threshold level is swept between -1.5dB and -0.9dB for each area with 0.05 dB of resolution (556 samples forested areas, 541 samples open areas, 9790 samples combined areas).

The variation of the accuracy within this range is not very significant. There is not a very clear minimum because the test was carried out with the complete set of images and therefore, as the threshold sweeps, it changes the group of images for those is most suitable. The table below shows the minimum acquired RMSE related to the thresholds levels:

Table 10, optimal threshold levels with 31 May 2005 image as reference

Area	Optimal Threshold	RMSE
Open	***-1.35 dB***	0.192
Forested	***-1.1 dB***	0.247
Combined	***-1.2 dB***	0.214

Table 10 shows that in this case the optimal levels are around -1dB which are assumed to be correct [3]. However, the RMSE evaluations are still poor, especially in forested areas. The poor accuracy may be caused by the influence of the forest canopy in the received signal.

26 May 2004 as reference image

The last detailed experimentation using *26 May 2004* as a reference image, is shown in Figure 15 representing 15 simulations and assessments for each area.

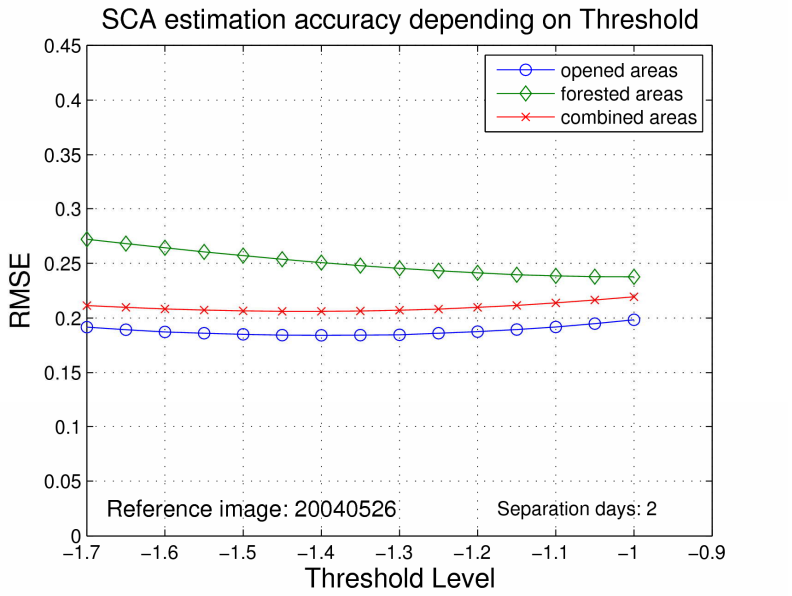

Figure 15, RMSE evolution when the Threshold level is swept between -1.7dB and -1dB for each area with 0.05 dB of resolution (525 samples forested areas, 506 samples open areas, 9148 samples combined areas).

The variation of the accuracy within this range is not very significant. There is not a very clear minimum because the test was carried out with the complete set of images and therefore while the threshold is swept, changes the group of images where is more suitable. The table below shows the minimum absolute RMSE related to the thresholds levels.

Table 11, optimal threshold levels with 26 May 2004 image as reference

Area	Optimal Threshold	RMSE
Open	***-1.4 dB***	0.184
Forested	***-1 dB***	0.238
Combined	***-1.45 dB***	0.206

Table 11 shows that in this case the optimal levels are around -1dB in forested areas and -1,5dB in open and combined areas, which are assumed to be correct [3]. The best SCA estimation accuracy was obtained using this image as reference.

4.2.2 Results using Dry Snow SAR images as reference data

The images acquired under dry snow conditions are also useful as reference in SCA estimation. However, the characteristics of the images might be not suitable because of the variables affecting the backscattering measurements. Unfortunately, there is only one image acquired under dry snow conditions, which was acquired on the 30th March 2005. The average backscattering levels are shown in Table 16 and it also compares them with the average, the minimum and the maximum values of the complete data set under study (Table 5).

Table 16, average backscattering for the image of 30 March 2005

Averaged Backscattering (dB)			
Reference Image	30 March 2005		
	Combined	Open	Forested
Averaged Value	-10.407	-11.204	-9.590
Averaged difference	**0.01**	**0.23**	**-0.2**
Minimum difference	1.50	2.18	0.83
Maximum difference	-1.62	-1.59	-1.64

The backscattering values obtained using 30 March 2005 image as reference, shown in Table 16, suggest inaccurate SCA estimation. The averaged difference is almost always positive, making it impossible to distinguish between this image from one acquired during the melting season. Figure 16 below shows the experimental searching of the threshold for the complete data set, representing 13 simulations and assessments for each area.

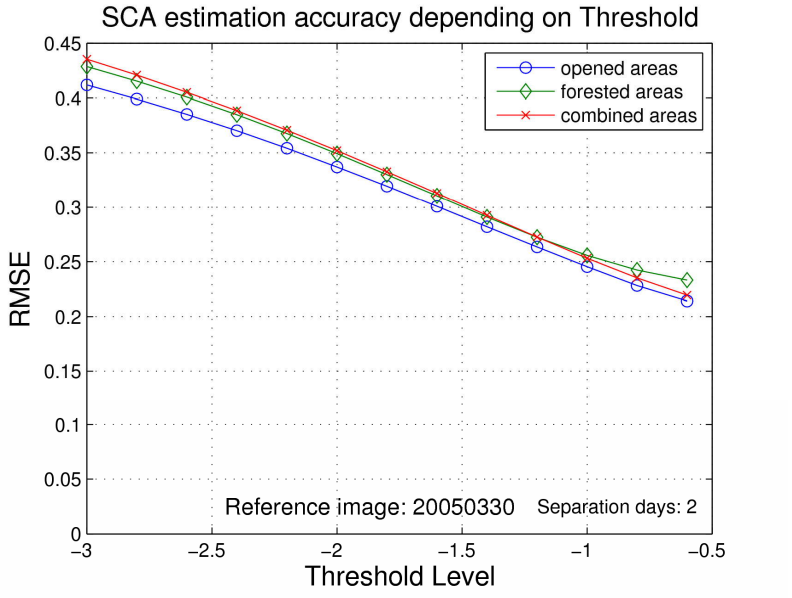

Figure 16, RMSE evolution when the Threshold level is swept between -3dB and -0.5dB for each area with 0.2 dB of resolution (557 samples forested areas, 540 samples open areas, 9172 samples combined areas).

The curve, in figure 16, follows a decreasing tendency while the threshold level is reduced. Therefore, the best results are acquired with a threshold close to zero, proving that the values of this reference image are too low to be useful in the discrimination process as predicted before. The main difference with the other reference images is that in this case the values obtained from forested and open areas are almost the same. This behaviour is also probably contributing to the poor SCA estimation accuracy achieved using these backscattering values as a reference. In conclusion, this image is useless in SCA estimation, although it is not reasonable to draw too far reaching conclusions upon the analysis of only one dry snow image.

4.2.3 Conclusions

- The best SCA estimation results are achieved using the reference image with lower averaged backscattering levels.

- The averaged backscattering level of the reference image has to be lower than the image under test in order to be able to produce a correct estimate.

- The difference between the average backscattering values of the reference image and the values of the complete data set approximates the suitable threshold level when the assessment is carried out that particular data set.

- The optimal threshold level changes progressively depending on the features of the image under study, making it impossible to determine the suitable threshold level by looking only at the reference image.

- The results showed better accuracy when the method is applied to estimate the SCA with data acquired from open areas. The results were inferior for forested areas.

4.3 Influence of the Analysed Image on the Threshold level

Up to this point the importance on the selection of the reference image has been evaluated looking at the accuracy of the estimates using the whole complete data set of images. Unfortunately, when the optimal threshold level was applied independently for each image, the results showed large discrepancy in the accuracies between the different SAR images. The results from these evaluations are listed in Table 17.

Table 17, independent accuracy for each image using a threshold of -1.45dB. Marked in grey is the unreliable data.

Image	Threshold (dB)	RMSE	Samples
30 April 2005	-1.45	0.153	353
28 April 2004	-1.45	0.247	1338
07 May 2005		No optical data available	
14 May 2005	-1.45	0.281	1299
12 May 2006	-1.45	0.206	263
12 May 2004		No optical data available	
02 May 2006	-1.45	0.178	1489
05 May 2004	-1.45	0.163	1455
05 May 2006	-1.45	0.185	1491
09 May 2006	-1.45	0.181	1460
26 May 2004		Reference Image	

In conclusion, the threshold level cannot be selected by only checking the features of the reference image. The variation in the data during the melt season should be the main selection criteria. The threshold level works by discriminating between the two kinds of surfaces based on a reference value during the melting process. The backscattering coefficients from these surfaces change depending on the weather conditions, the surface roughness, and the snow liquid water content [3]. Furthermore, the large area under study presents a noticeable variation between the data measured on the northern locations and the ones measured on the southern locations. These are some of the potential errors, reducing the estimation accuracy and complicating the discrimination process.

In the next phase, a search for the threshold level that yielded the least root mean squared error (RMSE) for each image was carried out. Table 18 presents this data along with the average difference on backscattering levels between the image and the reference. The average of the optical Modis SCA estimates used to evaluate the accuracy, are also indicated.

Table 18, optimal threshold for each image when individually compared with the SCA Modis estimates. There is also the averaged difference between the reference image and each image. Images organized by the backscattering value from the lowest to the greatest. Marked in grey are the unreliable data.

Image	Threshold (dB)	RMSE	Samples	Averaged Backscattering (dB)	Averaged difference (dB)	Averaged SCA MODIS
30 April 2005	**-1.1**	0.143	353	-12.027	-3.16	66 %
28 April 2004	**-0.5**	0.169	1338	-11.299	-2.43	83 %
07 May 2005	------No optical data available------			-10.692	-1.82	------
14 May 2005	**-0.5**	0.216	1299	-10.298	-1.43	64 %
12 May 2006	**-2.5**	0.087	263	9.839	-0.97	12 %
12 May 2004	------No optical data available------			-9.826	-0.95	------
02 May 2006	**-1.1**	0.170	1489	-9.655	-0.78	41 %
05 May 2004	**-1.7**	0.153	1455	-9.639	-0.77	29 %
05 May 2006	**-2.1**	0.161	1491	-9.524	-0.65	24 %
09 May 2006	**-2.5**	0.092	1460	-8.901	-0.03	7 %
26 May 2004	Reference Image			**-8.871**		

As seen in Table 18, when taking into consideration only the reliable data, the optimal threshold evolves inversely in regard to the averaged difference. The first impression when these calculations were carried out with the complete data set was that these values were closely related in the least RMSE conditions. However, this conclusion cannot be extrapolated to the particular case of each image. Respectively, the SCA estimates acquired by optical data also evolves inversely in regard to the optimal threshold level.

Using the Modis SCA estimates of each drainage basin of each SAR image, the backscattering values were classified as either dry or wet snow. After that their average backscattering levels and the standard deviations were calculated. The graphical representation is shown in Figure 17.

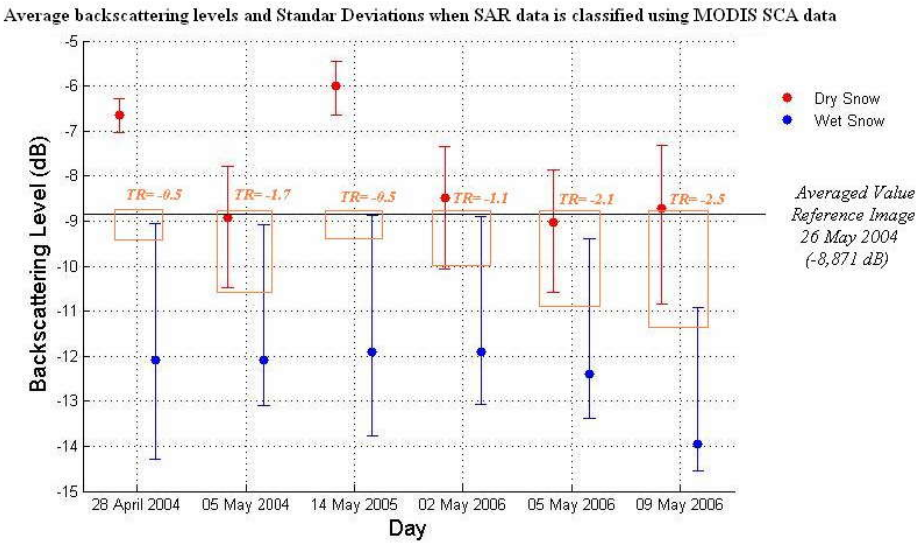

Figure 17, average backscattering levels and standard deviation of the dry snow (blue colour) and wet snow (red colour) areas. The orange box represents the suitable threshold level for each image listed in table 18.

Figure 17 can be used to interpret the results and the optimal threshold levels. There are two main cases, the first one being when the dry snow values are higher than expected, and the other one when these values are close to the reference image averaged values. Usually, the higher backscattering values either in dry snow or bare ground indicate an early stage in the melting process. As illustrated by Figure 17, the two images with these conditions are *28 April 2004* and *14 May 2005*. Checking the Modis SCA estimates it is realized that they have the greatest snow-covered area, 84% for the first and 64 % for the second image. The average value of the reference image is then quite small compared to these dry snow values because this data was acquired at the end of the melt season. Therefore, the discrimination process loses accuracy the higher the threshold level is, because the comparison is carried out by looking at the reference data. As a result, the simulations achieve the best results with threshold levels near zero. In the other hand, when the dry snow average values are similar to the reference image average, the optimal threshold level is directly related to the standard deviation (std).

An important relationship between the images *5 May 2004* and *5 May 2006* should also be noted. The interesting point is that both had very similar SCA conditions in spite of the 2 years time difference. In addition, both had also quite similar values for the dry and wet snow backscattering values and, as a consequence, the optimal threshold level is almost the same. The evolution during the melt season of 2006 is also important. Probably this is the most clear available data, showing how the averaged and maximum deviation of the averaged values of wet snow decreases as the season progresses whereas the value of dry snow remains almost stable. As a consequence, the optimal threshold level follows a decreasing tendency reaching a lowest value near -3dB.

The following figures compare the estimates made for each of the images listed in Table 18 with the Modis SCA data. The main distribution of the values, as well as the values of SCA estimates which produce more errors can be extracted from here.

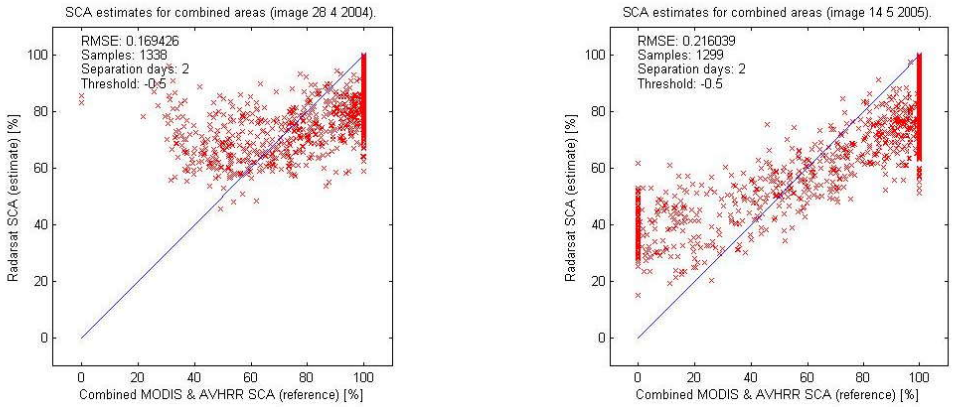

Figure 18, estimated SCA values plotted in comparison with reference SCA data. The SAR images are acquired on 28 April 2004 and 14 May 2005. Both images produced the best results using a threshold level of -0.5dB

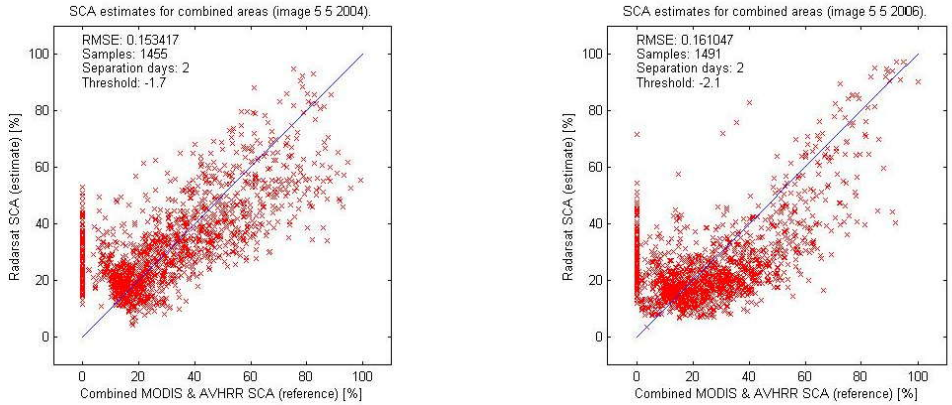

Figure 19, estimated SCA values plotted in comparison with reference SCA data. The SAR images are acquired on 5 May 2004 and 5 May 2006. Both images had similar conditions.

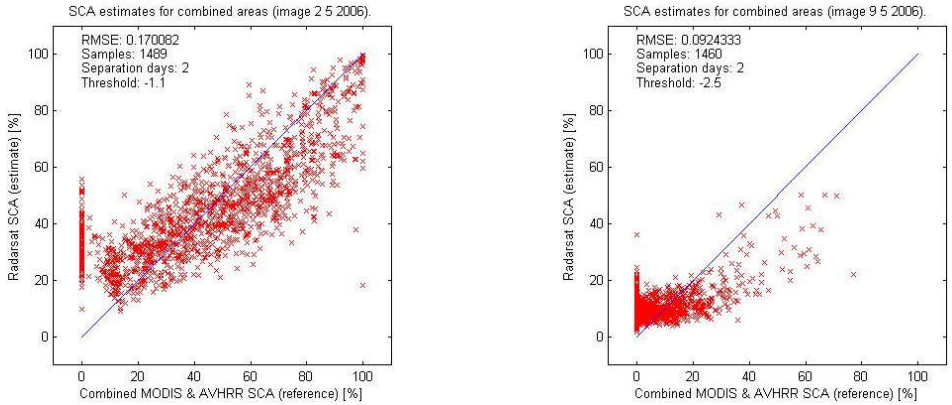

Figure 20, estimated SCA values plotted in comparison with reference SCA data. The images are acquired on 2 May 2006 and 9 May 2006. Both images were acquired during the same melting process.

The next step in the analyses was to evaluate the contributions depending on the geographical area. The locations across the complete area under study experience different conditions, during the melting season, thus increases the variations in the data. Therefore, the averaged values are dependant on the location.

Conclusions

- The wet snow backscattering values have a high standard deviation, and for some areas reach values greater than the averaged value from the reference image, this makes the discrimination impossible.

- Using references images acquired at the end of the melt season (bare ground conditions) requires low threshold levels because of the contributions of the dry snow pixels at the beginning of the melt season usually have higher backscattering values.

- The suitable threshold level is directly related to the image under study. In fact, it follows a decreasing tendency while the melting season progresses. Therefore a unique value for the complete data set will result in poor estimation accuracy.

4.4 Evaluation of the Backscattering Contributions Depending on the Area

In the previous section the variation of the suitable threshold values during the melting process was evaluated. All the results up to this point have been related to the averaged backscattering from all of the northern Finland. This region covers more than 100000 km^2 and the distance between the northern and the southern areas is more than 500 km. Consequently, the weather is different and the melting process does not start at the same time within the different regions. In this context, it explains the standard deviation of the observed backscattering values. Figure 21 shows the distribution of the 2037 drainage basins under study.

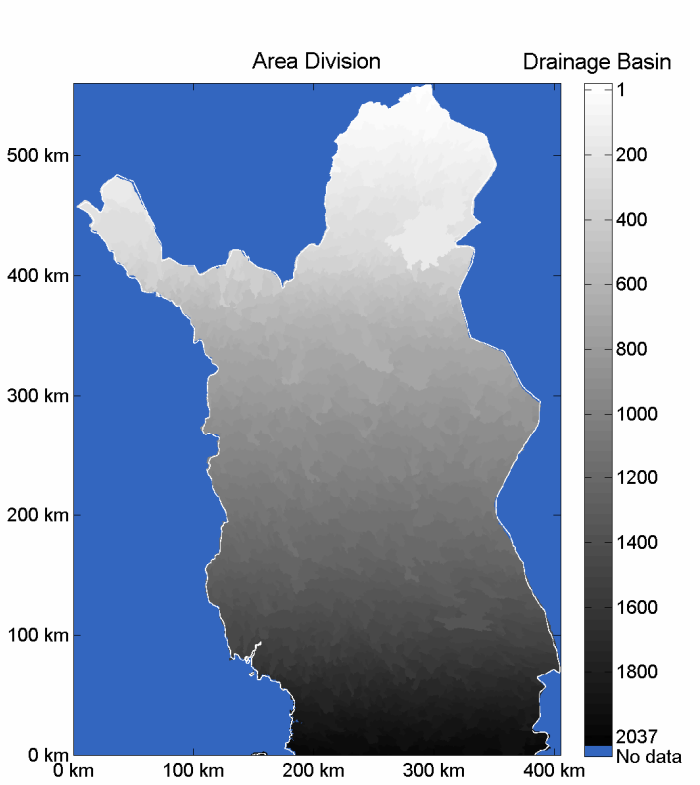

Figure 21, drainage basin distribution in northern Finland represented using grey scale criteria. The distance scale is also indicated.

The backscattering values extracted from the SAR images were classified by examing the optical Modis SCA data independently for each drainage basin (Section 2.6). The SCA estimates were calculated as a value for each drainage basin using the available pixel information inside each area. Once the SCA value is known and the algorithm used in the SAR estimation (Section 2.7.2) taken into account, it is easy to classify each pixel into either dry/bare ground or into wet snow. This provides good information about the variation of both kinds of data independently for each location. This was carried out for all suitable images from the 2006 season in order to analyse the evolution during one melting season as well as for the reference images.

4.4.1 Evolution inside the *2006* data set

The Figure 22 shows the SCA estimates acquired with MODIS optical data for all the drainage basins under study. The evolution during the melting period is clearly observed: the SCA estimate decreases for all the locations as the melting season progresses. It is also noted that the highest reduction was in the northern areas (lowest value in the drainage basin classification), where the snow-covered area was almost 60% on *2 May 2006* and less than 20% on *9 May 2006,* with only 7 days of difference. On the other hand, the reduction inside the southern areas was much lower, approximately 20 percentage units over the same period of time.

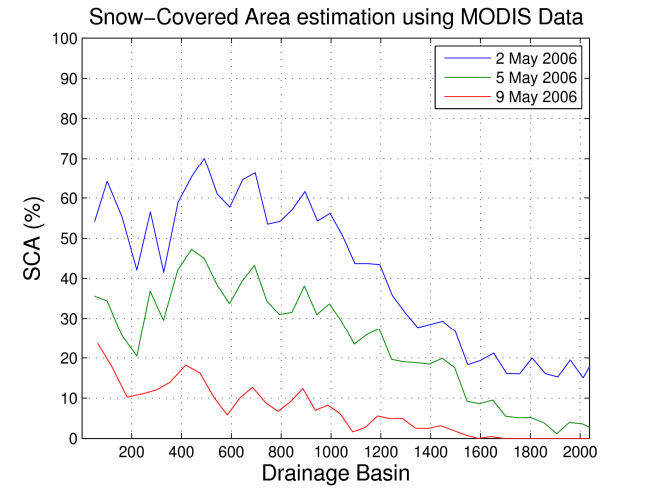

Figure 22, SCA Modis estimates depending on the drainage basin for the available data of 2006. The curve has been created by averaging the data of 50 drainage basins.

The backscattering coefficients of the drainage basins for each image during the melting process of 2006 are shown in Figure 23. The values for the reference image used in the analyses are also represented.

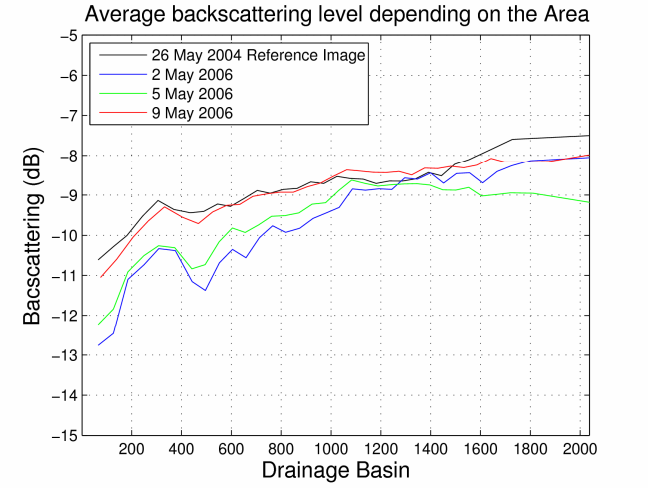

Figure 23, the backscattering levels depending on the drainage basin for the available data of 2006. The curve has been created by averaging the data of 50 drainage basins.

Comparison of the Figures 22 and 23 shows the greater reduction of the values inside the areas more covered by snow during the melt season whereas the backscattering values for the southern areas are higher. Essentially, this behaviour is directly related to the amount of pixels in the analysed area showing bare ground or wet snow. For this reason, the northern areas have lower values because they are dominated by wet snow pixels. The evolution during the melting period is also clearly noted, the earliest image showing the lower values which increase proportionately in the next images, maintaining generally, the shape of the curve. However, a reduction it was noted in the values of the image *5 May 2006* for the southern drainage basins whereas the other two images have similar values. The main reason for this deviation is that the area is dominated by bare ground pixels, and the *5 May 2006* image was acquired with an incidence angle of almost 10° greater than the other images. In other words, the levels are lower because of the increase on the incidence angle.

The averaged values of the bare ground pixels were also calculated independently for each drainage basin and are presented in Figure 24.

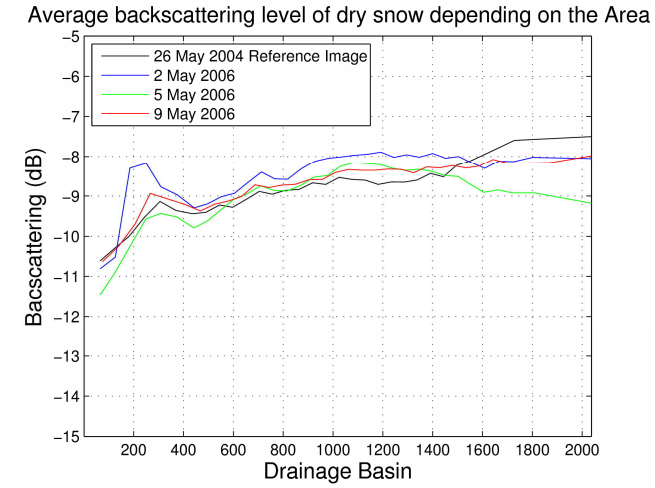

Figure 24, the backscattering levels of dry snow and bare ground depending on the drainage basin for the available data of 2006. The curve has been created by averaging the data of 50 drainage basins.

Figure 24 shows the evolution of the bare ground pixels contribution, during May. It is important to note the small difference throughout the melt season, when compared to the reference image corresponding to May 2004. In fact, the reference image curve is quite similar for most of the areas, especially the ones which are still melting, because the ground is probably still wet [10].

The in-sight learned from the analyses thus far, was that the behaviour of the bare ground values were quite similar inside the same drainage basin, at least in the final stage of the melting process. Therefore, the threshold level is not significantly affected by the variation of the coefficients from the bare ground within the area under study. In this respect, the contributions from wet snow pixels become important in the determination of the discrimination or threshold level.

For the analysis of the results, the next step was the evaluation of the wet snow contributions depending on the drainage basin. Figure 25 shows the results.

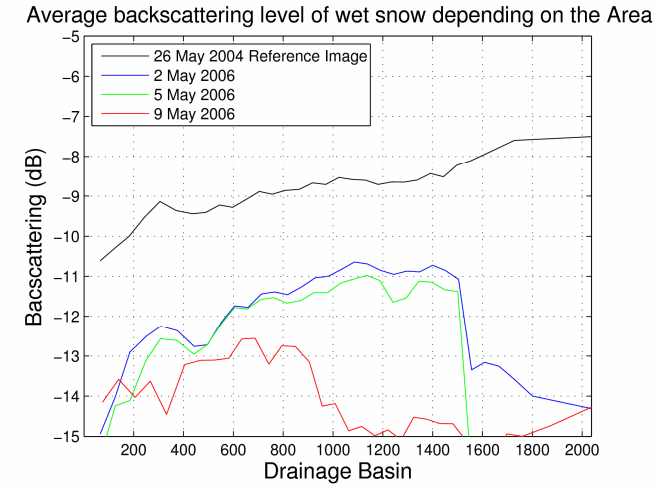

Figure 25, the backscattering levels of wet snow depending on the drainage basin for the available data of 2006. The curve has been created by averaging the data of 50 drainage basins.

The wet snow data shows the greatest variation in this data set. In general, this is the most important information that can be used for predicting the melting process. The highest backscattering values were measured for the earlier image and then the values started to decrease almost proportionally, reaching the lowest level on the final image. The variation inside this data is great, also for each drainage basin reaching in some cases values close to -9dB; this, evidently, is the main source of error in the estimates. Comparing Figure 25 to the data shown Figure 17, it is noticed that the threshold level increases when the overall amount of wet snow pixels is reduced. In other words, the threshold level decreases while the melting season is underway. However, as shown in Figure 22, the evolution of the melting process is quite different for each sub-area and, as a consequence; the suitable threshold level should not be the same for the complete region under study.

4.4.2 Comparison between the reference images

The backscattering coefficients of the reference image are the core of the estimation. In Section 4.3 the accuracy obtained using each image was analysed and the relationship of these results with the average level of their backscattering coefficients was demonstrated. In this connection there the evolution of the backscattering values within the complete area was also calculated. Figure 26 presents these results.

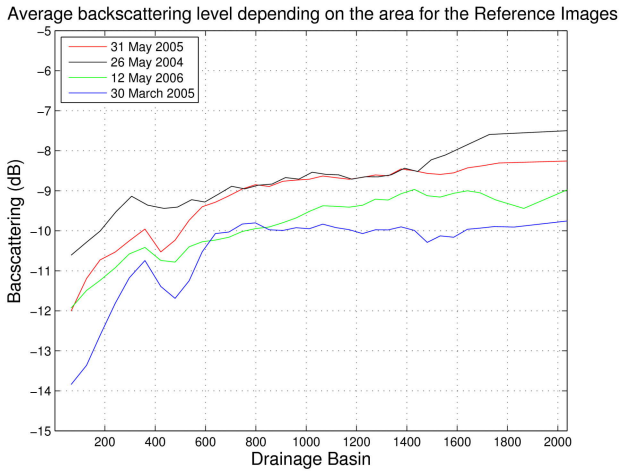

Figure 26, the backscattering levels depending on the drainage basin for the reference images. The curve has been created by averaging the data of 50 drainage basins.

The graphic shows that the reference image of *26 May 2006* had the highest backscattering values for all the areas in spite of the fact that the image acquired on *31 May 2005* had almost the same values for some areas. The most significant information given by this representation is that the shapes of all the curves are quite similar, increasing or decreasing in the same areas for different years. Moreover, the lower differences are situated in the northern areas where the melting process ends later and the ground was probably still wet. As a consequence, the backscattering values were higher [10]. The highest differences are probably related to the variation in the incidence angle. In fact, the image with highest backscattering values was acquired with an incidence angle of 25.7º, the next highest with 30.9º, and the last two with an incidence angle of 36.1º. In summary, the differences between these images are primarily caused by variations of the incidence angle, due to the fact that the bare ground and the dry snow backscattering levels are widely affected by this variation [3].

4.4.3 Influence of an areal Threshold level on SCA estimation Accuracy

In the previous pages the high variation of the backscattering values along the large area under study, related to the variation of the incidence angle, the forest stem volume and most importantly, the moment during the melting process has been demonstrated. All of these factors make the selection of a unique threshold for the complete study area of northern Finland quite difficult. Therefore, the study area was divided into smaller sub-areas by taking into account the behaviour of the backscattering coefficients within the drainage basins for the different years. The complete area was divided in 5 smaller areas represented with different colours in Figure 27.

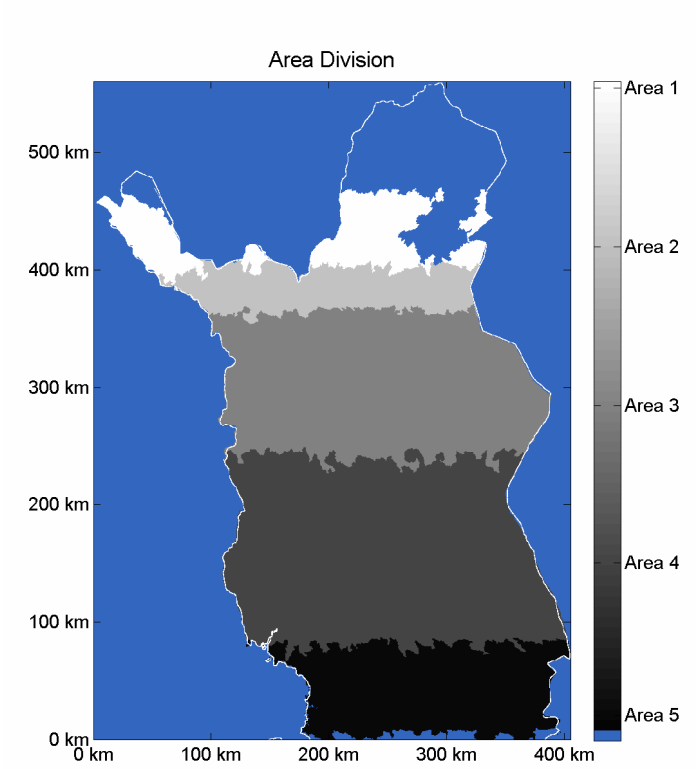

Figure 27, division of the study area of northern Finland represented using grey scale criteria. The distance scale is also indicated.

Table 19, division of the study area and drainage basins range included within each area

Area Division	
Area	*Drainage Basins included*
1	200 - 400
2	400 - 600
3	600 - 1000
4	1000 - 1600
5	1600 - 2000

The data set used is the same as presented in Section 4.3 having as reference, the image acquired on *26 May 2004*. The Table 20 shows the images used in the accuracy analysis, along with the best threshold level for each one.

Table 20, utilized data set, and the optimal threshold level for each image.

Image	Threshold (dB)
28 April 2004	**-0.5**
05 May 2004	**-1.7**
14 May 2005	**-0.5**
02 May 2006	**-1.1**
05 May 2006	**-2.1**
09 May 2006	**-3**

The optimal threshold level for each area was identified and used to calculate the SCA estimates for each area. The final SCA estimates of the complete image were combined from the different parts. The most suitable threshold values for each image and area are presented in Figure 28:

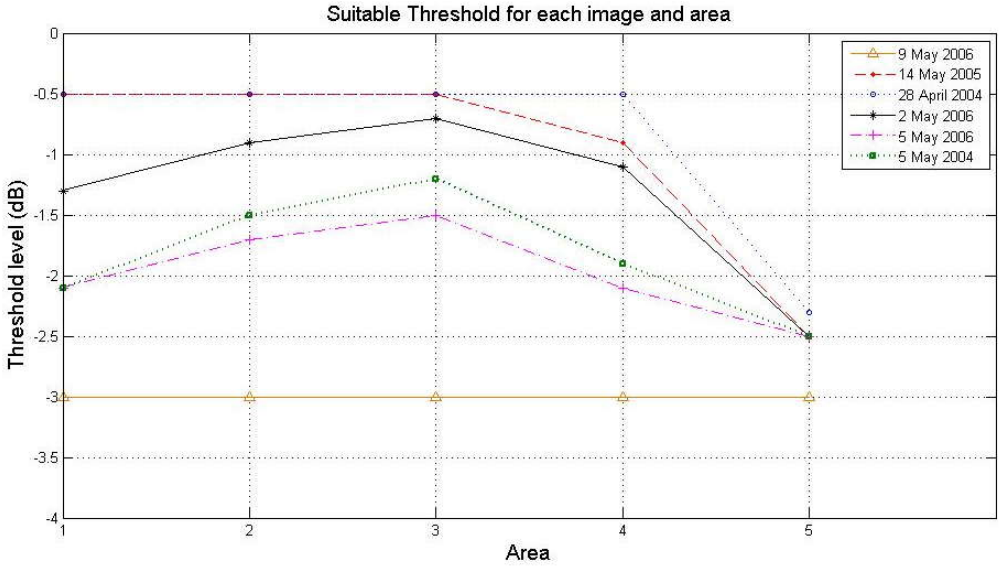

Figure 28, optimal threshold level determined by the RMSE for each image and area

The results in Figure 28 are quite important. The first obvious point is the overall variation and reduction of the threshold value for all the areas while the melting season is underway. This is a strong reaffirmation of the prior conclusions. Moreover, the images in the middle of the melt season follow the same tendency in the threshold values for all the years. In other words, from knowing the suitable value of one area can be forecasted approximately the correct value for the other areas.

Once the optimal threshold values for each area were identified, the new SCA estimates were analysed by comparing them with the optical reference data. Table 21 shows the assessment using the data set listed in Table 20. The table also shows the RMSE values achieved in the section before considering a different threshold value for each one of the images under analysis (Section 4.3).

Table 21, comparison of the best accuracies obtained by using a unique or variable threshold for large areas.

Accuracy assesment		
	RMSE	Samples
Unique Threshold *(The same for all images)*	***0,206***	8532
Unique Threshold *(different for each image)*	***0,163***	8532
Variable Threshold	***0,146***	8532

The results clearly demonstrate that the degree of accuracy is better when the area under analysis is taken into account. The Table 22 shows the results when the evaluation is carried out independently for each image.

Table 22, comparison of the best accuracies obtained by using a unique or variable threshold for large areas independently for each image.

Accuracy assesment			
Image	**RMSE**		**Samples**
	Unique Threshold	Variable Threshold	
28 04 2004	***0,169***	***0,156***	1338
05 05 2004	***0,153***	***0,132***	1455
14 05 2005	***0,216***	***0,192***	1299
02 05 2006	***0,17***	***0,148***	1489
05 05 2006	***0,161***	***0,144***	1491
09 05 2006	***0,092***	***0,089***	1460

All the new SCA estimates show enhanced accuracy, demonstrating the importance of the division of the study area when choosing a suitable threshold level.

4.4.5 Conclusions

- The accuracy of SCA estimation is reduced if a single threshold level is utilized for large areas. If the threshold value is selected independently for each small area, the estimation accuracy improves.

- The variation of the threshold level between the different areas in northern Finland is usually similar during the snow-melt season.

- The increase of the incidence angle decreases the backscattering values in general which affects the images used as reference, in particular, making the images with high incidence angle unusable in the SCA estimation process.

- The local behaviour of the average backscattering values between different years with similar SCA conditions was observed.

4.5 Adaptation of Nagler & Rott Method for Northern Finland

The results up to this point were achieved through analysis of large groups of estimation results and extracting the best ones. This techniques, however, requires prior knowledge of the correct estimates in order to compare and evaluate the accuracy. Essentially, the objective after all the evaluations is to be able to design a method useful for generating the SCA estimates without almost any reference data, while still obtaining highly accurate results. In this context, the algorithm presented by Nagler & Rott [3] (Section 2.7) is still used as the core for the SCA estimation. However, the threshold value has to be managed in the adapted method, since the analyses show a high variation of the suitable value depending on the time and the area.

The reference image could be selected as a part of the process, but the image acquired on 26 May 2004 showed the best accuracy for all the different annual estimates and was selected as the reference image. In fact, this image has the best features, meaning the highest threshold level, and therefore, can be used as reference for various data sets. The main process includes two steps: the first one determines a universal threshold for the complete area of northern Finland; and the second calculates the threshold to be used for each of the smaller areas (Figure 27).

4.5.1 First step

The first step selects a threshold level for the study area based on the most recent acquired MODIS SCA estimates. Usually the value of the threshold level decreases as the melting season progresses (Section 4.3). Therefore, this value can be estimated by examining the averaged SCA value as indication of the current instance of snow-melt season. Generally, it was noticed that the values swung between -0.5dB and -3dB (Section 4.3). The decision rule is presented in Figure 29.

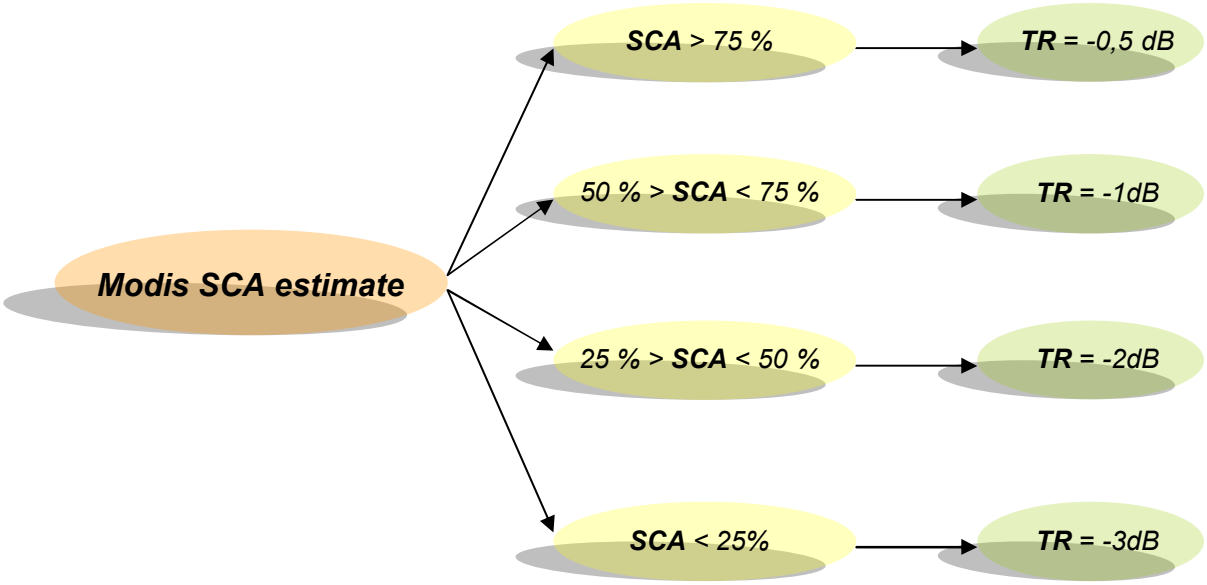

Figure 29, rules for the threshold level selection based on the SCA MODIS data

4.5.2 Second step

The second step takes into account the division shown in Figure 27, where the study area of northern Finland is divided into 5 sub-areas. The threshold level decided on the first step is used to determine the threshold level of the main area, which is referred to as area 4. Hence, if the image moment is in the middle of the snow-melt season, a different threshold is decided for each area. Otherwise all the areas use the same main threshold value. The decision rules are presented in the Figure 30:

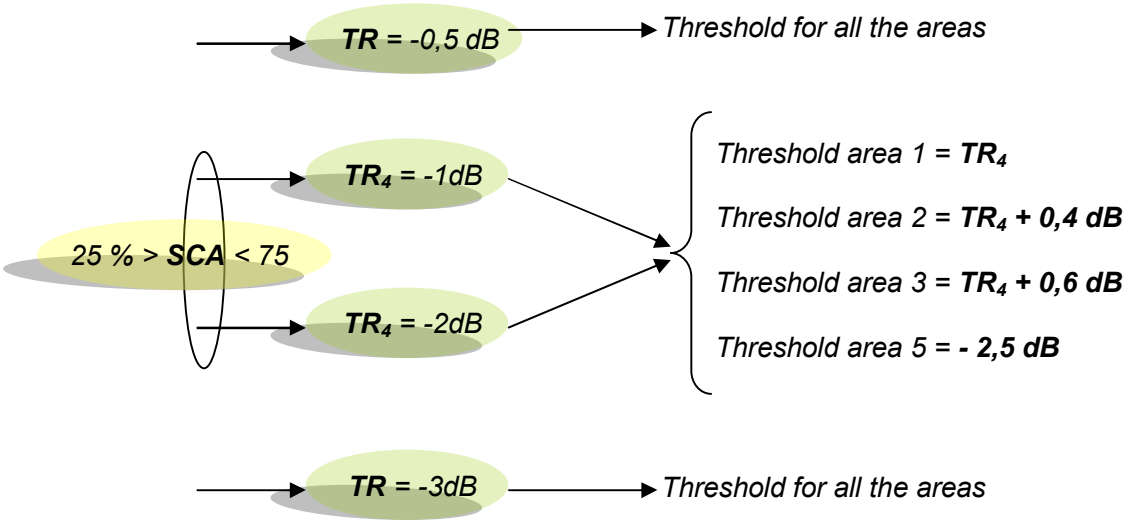

Figure 30, rules for the threshold level selection for the different areas

4.6 Comparison of the Accuracy with the TKK Method

4.6.1 Numerical Comparison

The main objective of this study was to compare the accuracy of the Nagler & Rott method to the current TKK method in northern Finland (Section 4.5). The peculiarities of these areas and the data set have been explained in earlier sections of this project, and all the evaluations have been carried out and widely explained in Sections 4.2 to 4.4. The main differences between both methods were the working topographical and geographical areas that each one was designed for. Furthermore, the Nagler & Rott method was implemented at the most elementary level, without the enhancements developed for the TKK method; primarily, the forest compensation and the weather station assimilation. The results of the Nagler & Rott method shown below, were achieved using the reference image acquired on *26 May 2004*.

The first comparison is between the results achieved with the baseline of the TKK method to the Nagler & Rott method using the suitable threshold level described in their algorithm (-3dB) [1]. The evaluation is shown for the complete data set in Table 23.

Table 23, comparison between the accuracies of the TKK and Nagler & Rott methods, carried out in the basic mode and taking into account the complete data set.

Root Mean Squared Error (RMSE)		
	RMSE	Samples
TKK method *(old base line)*	**0.151**	9020
Nagler & Rott	**0.307**	9148

Obviously, the level of accuracy obtained using the Nagler & Rott algorithm was insufficient and noticeable worse than the results achieved using the current TKK method. Therefore, the search for the most suitable threshold level was conducted in order to determine the two step Nagler & Rott method adapted to northern Finland (Section 4.5). The first step selects a threshold level for each image depending on the last SCA Modis estimation, which in this study is compared to the TKK method with the weather station assimilation. This data is included in the Table 24, which refers to the data acquired each year and also to the complete data set.

Table 24, comparison between the accuracies of both methods: The Nagler & Rott method adapted to northern Finland (Section 4.5) applying the first step (an independent threshold for each image); and the TKK method with the addition of the weather station assimilation. The results are split into different years and shown also for the complete data set.

Root Mean Squared Error (RMSE)				
Nagler & Rott (One Step)	2004	2005	2006	Complete dataset
RMSE	**0,164**	**0,247**	**0,181**	**0,188**
Samples	2793	1299	4440	8532
TKK method (WSA)				
RMSE	**0,128**	**0,172**	**0,135**	**0,139**
Samples	2772	1628	4620	9020

The results with the adapted Nagler & Rott algorithm (one step, Section 4.5.1) again showed worse accuracy than the TKK method. However, at this point the difference is not as significant as in the previous evaluation. It was also noted that both methods achieved the greater results for the 2006 data set and the worse results for the 2005 data set. Furthermore, the results showing best correlation were obtained for the 2004 data set, with the difference being approximately 0.04.

The final evaluation was to compare the latest enhanced method developed at TKK with the improved Nagler & Rott method which decides a different threshold level for the different areas under analysis (Section 4.5.2). The results are shown in Table 25.

Table 25, comparison between the accuracies of both complete methods, the results are split into different years and also shown for the complete data set.

Root Mean Squared Error (RMSE)				
Nagler & Rott (Two steps)	2004	2005	2006	Complete dataset
RMSE	**0,152**	**0,211**	**0,168**	**0,170**
Samples	2793	1299	4440	8532
TKK method (Current)				
RMSE	**0,115**	**0,158**	**0,115**	**0,123**
Samples	2772	1628	4620	9020

The results showed one more time, a worse level of accuracy for the Nagler & Rott method for all the analysed data. Nevertheless, it is important to note the improvement in the accuracy of the results using the Nagler & Rott method after applying the second step (Section 4.5.2), comparing between the results of tables 24 and 25.

4.6.2 Graphical representation of the SCA estimation accuracy

Once the numeric results have been presented it is also interesting to see the graphical representations of the estimated values as a function of the MODIS SCA estimates. Essentially, each figure represents the SCA estimates acquired with the adapted Nagler & Rott method (located on the left) and the SCA estimates acquired with the enhanced TKK method (located on the right), for each year and also for the complete data set.

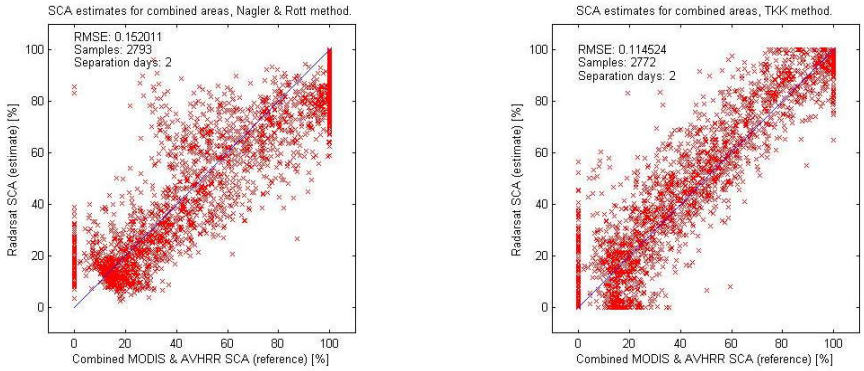

Figure 31, estimated SCA values acquired using the TKK and Nagler & Rott methods for the 2004 data set compared with MODIS SCA data

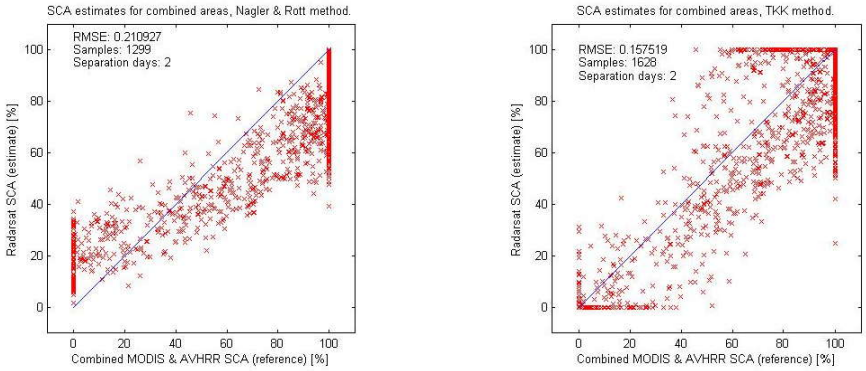

Figure 32, estimated SCA values acquired using the TKK and Nagler & Rott methods for the 2005 data set compared with MODIS SCA data

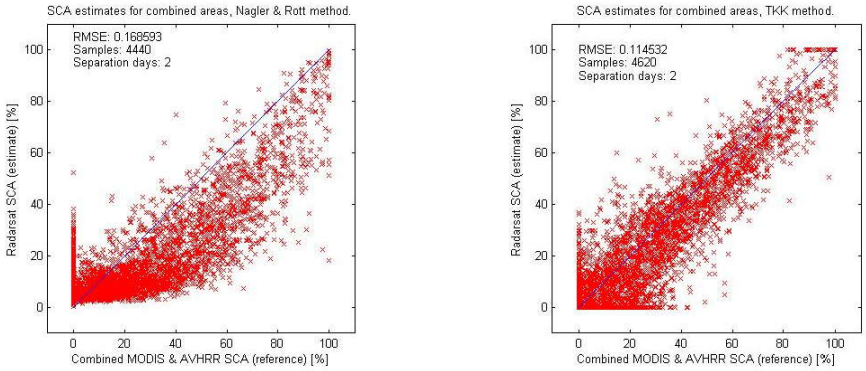

Figure 33, estimated SCA values acquired using the TKK and Nagler & Rott methods for the 2006 data set compared with MODIS SCA data

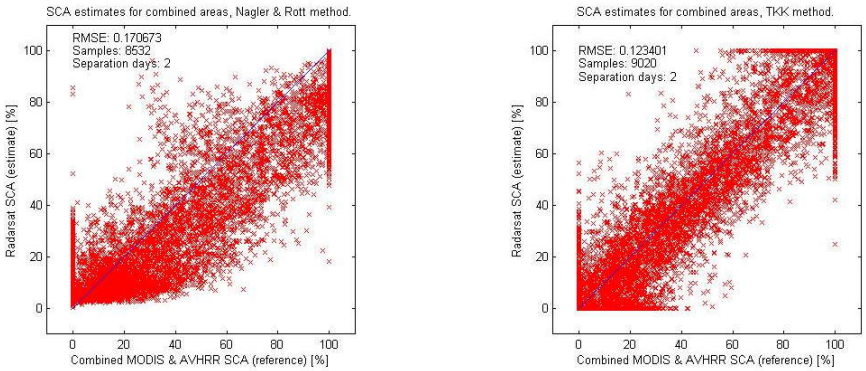

Figure 34, estimated SCA values acquired using the TKK and Nagler & Rott methods for the complete data set compared with MODIS SCA data

The correlation plots of Figures 31, 32, 33 and 34 confirm again the higher accuracy of the TKK method. In fact, those estimates show a more linear pattern of behaviour along all the SCA values than those acquired using the Nagler & Rott method. In general, the distributions of the values estimated with the Nagler & Rott method are lower than the expected values, however, never quite reaching the 100% or 0% SCA value. In this context both methods produce significant errors when the Modis estimates are 100% or 0%, but only the TKK method makes many wrong estimates by deciding 100% or 0% when the Modis values are different. A comparison between the maps generated by both methods is included in Appendix II.

4.6.3 Conclusions

- The evaluations have shown the superiority of a method based on two reference images over the method based on only one, on the study area of northern Finland.

- The effect on the backscattering values of the large forested areas, compensated in the TKK method, yields a great amount of errors in the application of the Nagler & Rott method.

- The TKK method do not needs the optical SCA MODIS data to function whereas the Nagler & Rott method can not work if the optical data is not available.

- The high level of accuracy achieved with the TKK method during the last stages of the snow-melt season is due to the application of weather station data, which is a noticeable difference between the two methods evaluated.

5 Summary and Conclusions

The main objective of this Final Project was to simulate and evaluate the statistical accuracy of the Nagler & Rott Snow Covered-Area estimation method in northern Finland to compare it with the current TKK SCA estimation method. Moreover, this study demonstrates the lower degree of accuracy obtained when a method developed for alpine areas is directly implemented in a region with different characteristics. Furthermore, the large area included in the analysis affected the results, making necessary the development of some selection rules in order to be able to compare the accuracy of both methods, showing finally the greater accuracy of TKK method.

The Radarsat images acquired between 2004 and 2006 were the analysed data set, being 14 images where each one covered more than 100000 Km^2 divided into 2037 drainage basin. The evaluations were carried out by comparing these data with the SCA estimates based on optical data (Chapter 3). The evaluation process was presented in Chapter 4, where the main goal was to determinate the conditions where the Nagler & Rott method achieve the best accuracy allowing the development of a newer method to adapt it to northern Finland.

The examination of the reference image selection (Section 4.2) was the initial point. The accuracy obtained by using 4 different images, with different conditions, is presented and related to the simulations carried out with different threshold levels. However, a concrete reference image selection procedure was not defined, although the results were always better when using as reference the image with lower averaged backscattering levels, probably because of the effect of the incidence angle (Section 4.4.2).

The next step in this analysis procedure was to evaluate the influence of each image under study independently (Section 4.3). In fact, this showed the direct relation between the threshold level and each image, proving the selection of a global threshold value inaccurate for the complete data set. The progressive variation of this level along the melting process was also noted, starting with the greatest value and ending with the lowest value.

The following evaluations (Section 4.4) concerned the influence of the different areas included in northern Finland. Essentially, the results showed the best estimation accuracy when the threshold level was selected independently for smaller areas. Consequently, the complete area was divided into 5 smaller areas where the drainage basin behaviour analysed was similar for many years. Furthermore, the variation of the suitable threshold level, during the melting process, between the 5 areas was similar for each year, allowing the estimation of each area's threshold level by examing the features of the greater area.

The adapted method to northern Finland was developed in Section 4.5 in order to be able to compare it to the current TKK SCA method. This new method is based on the conclusions reached after all the evaluation processes up to this point. First, the algorithm determines the threshold level of the greater area by looking at the optical based SCA estimates. Once it is

solved, the threshold for the remaining areas is selected following rules of the second step (Section 4.5.2).

The last section in Chapter 4 shows the comparison between the results achieved by both methods using the same data set. In all the cases, the TKK method was superior being more reliable. The first estimations compared were the base line of the TKK method to the Nagler & Rott method using the -3db threshold proposed in their article. Two further comparisons were carried out for each one of the steps in the adapted new Nagler & Rott method. These were measured against the TKK method with only the weather assimilation enabled as well as with the complete current method developed TKK.

References

Documents

[1] T. Nagler and H. Rott, Retrieval of Wet Snow by Means of Multitemporal SAR Data, IEEE Trans. Geosci. Remote Sensing vol.38, no.2 ed., Austria: S 0196-2892, 2000.

[2] K. Luojus**,** J. Pulliainen, S. Metsämäki, G. Molera, R. Nakari, J-P Kärnä, and M. Hallikainen, Development of SAR Data-Based Snow-Covered Area Estimation Method for Boreal Forest Zone, Proceedings of IEEE 2008 International Geoscience and Remote Sensing Symposium (IGARSS'08), Boston, Massachusetts, USA, 6-11 July 2008.

[3] R. Magagi, M. Bernier, Optimal conditions for wet snow detection using RADARSAT SAR data, Remote Sensing of Environment 84 ed. , Quebec: Elsevier, S0034-4257, 2002.

[4] K. Luojus, and J. Pulliainen, Automatic Processing Chain for SAR Data-Based Snow-Covered Area Estimation Method, Helsinki University of Technology, Laboratory of Space Technology, Report No. 65, Espoo, Finland, November 2006.

[5] C. Oliver, S. Quegan, Understanding Synthetic Aperture Radar Images, Norwood: ARTECH HOUSE, INC, 1998.

[6] W. Gareth, Remote Sensing of Snow and Ice, Boca Raton: Taylor & Francis Group, 2006.

[7] K. Luojus, Master's Thesis**:** Snow Covered Area Estimation Using Spaceborne Radar, Helsinki University of Technology, Department of Electrical and Communications Engineering, Finland, June 2004.

[8] K. Luojus, Licentiate Thesis**:** Operational Snow-Covered Area Estimation for Boreal Forest Zone Using Spaceborne Radar, Helsinki University of Technology, Department of Electrical and Communications Engineering, Finland, February 2007.

[9] Sari J. Metsämäki, Saku T. Antilla, Huttunen J. Markus, Jenni M. Vepsäläinen, A Feasible Method for Fractional Snow Cover Mapping in Boreal Zone Based on a Reflectance Model, Finland: Elsevier, 2004.

[10] T. Koskinen, T. Pulliainen, T. Hallikainen , The Use of ERS-1 SAR Data in Snow Melt Monitoring , IEEE Trans. Geosci. Remote Sensing vol.35, no.3 ed., Espoo: S 0196–2892/97, 1997.

[11] Radarsat International, RADARSAT Data Products Specifications, 3/0 ed., Canada: n.p., 2000.

[12] N. Baghdadi, Y. Gauthier, and M. Bernier, Capability of Multitemporal ERS-1 SAR Data for Wet-Snow Mapping, Remote Sens. Environ. 60:174-186 ed., Québec, Canada: Elsevier, 1997.

[13] N. Baghdadi, Y. Gauthier, M. Bernier, and J. Fortin, Potential and Limitations of RADARSAT SAR Data for Wet Snow Monitoring, Remote Sens. Environ. vol. 38, no. 1 ed. , Québec, Canada: S 0196-2892, 1998.

[14] A. Langlois, D.G. Barber, B.J. Hwang, Development of a winter snow water equivalent algorithm using in situ passive microwave radiometry over snow-covered first-year sea ice, Remote Sens. Environ. 106, 75-88 ed. , Canada: elsevier, 2006.

[15] M. Hallikainen, F. Ulaby, and M. Abdelrazik, Dielectric Properties of Snow in the 3 to 37 GHz Range, IEEE Trans. on Antennas and Propagation. vol. AP-34, no. 11 ed. , Finland: 0018-926X, 1986.

[16] J. Koskinen, S. Metsämäki, J. Grandell, S. Jänne, L. Matikainen, and M. Hallikainen, Snow Monitoring Using Radar and Optical Satellite Data, Remote sens. Environ. 69:16-29 ed. , Finland: Elsevier, 0034-4257, 1999.

[17] J. Koskinen, J. Pulliainen, J. Hyyppä, M. Engdahl, and M. Hallikainen, The seasonal Behavior of Interferometric Coherence in Boreal Forest, Trans. Geosc. Remote Sensing, vol 39, no. 4 ed. , Finland: 0196-2892, 2001.

[18] T. Nagler, and H. Rott, SAR Tools for Snowmelt Modelling in the Project HydAlp, Innsbruck: 0-7803-4403-0, 1998.

[19] J. Pulliainen, Mapping of snow water equivalent and snow depth in boreal and sub-artic zones by assimiating space-borne microwave radiometer data and ground-based observations, Remote Sensing of Environment. 101, 257-269 ed. , Espoo: 0034-4257, 2006.

[20] J. Shi, J. Dozier, Estimation of Snow Water Equivalence Using SIR-C/X-SAR, Part II: Inferring Snow Depth and Particle Size, Transac. Geoscienc. and Remote Sensing, vol. 38, no. 6 ed. , California: 0196-2892, 2000.

[21] T. Ault, K. Czajkowski, T. Benko, J. Coss, J. Struble, A. Spongberg, M. Templin, C. Gross, Validation of the MODIS snow product and cloud mask using studend andNWS cooperative station observations in the Lower Great Lakes Region, Remote Sensing of Environment, 105, 341-353 ed. , United States: elseiver, 2006.

[23] B. Vehviläinen, The watershed simulation and forecasting system in the National Board of Waters and Environment, No.17 ed. , Finland: Publications of the Water and Environment Research Institute, 1994.

Images

***Figure 1*:** Reprinted from Engineering & Science, spring 1991, v. LIV, no. 3, p. 16

***Figure 2*:** Radarsat International, RADARSAT Data Products Specifications, 3/0 ed, Canada: n.p., 2000.

***Figure 3*:** K. Luojus, Snow Covered Area Estimation Using Space-Borne Radar, Espoo: Helsinki University of Technology, 2004.

***Figure 4*:** R.Magagi, M. Bernier, Remote Sensing of Environment , 84 (2003) 221-233

Figure 5, 6 and ***9***: K. Luojus, J. Pulliainen, S. Metsämäki, G. Molera, R. Nakari, and M. Hallikainen , Enhanced SAR Data-Based Snow-Covered Area Estimation Method for Boreal Forest Zone, Espoo: 2007.

***Figure 7*:** T. Nagler and H. Rott, Retrieval of Wet Snow by Means of Multitemporal SAR Data, IEEE Trans. Geosci. Remote Sensing vol.38, no.2 ed. , Austria: S 0196-2892, 2000.

APPENDIX

Appendix I SCA_nagler Matlab Script

```
% ---------------------------------
% TKK, Space of technology laboratory
% Alberto Blasco, 13.02.2008
% SCA estimation based on Radarsat data
%
%
% procstep_4_SCA_nagler.m

function sigma0_calc = procstep_4_SCA_nagler(hakemisto,ref_image,TR,Pixels,mode)


Alueita=2037;  %Number of Drainage basins
Limit=10^(TR/10);

image_1=['sigma0\',hakemisto,'_CAL_REC_50_final_100m.mat'];   %Image
provided by RADARSAT
image_ref=['sigma0\',ref_image,'_CAL_REC_50_final_100m.mat'];  %Reference
Image(Bare_ground or dry_snow)
valuma_file='reference_data\refdata_ykj_drainagebasin_100.mat'; %Correct
Region and location of each Drainage Basin
slam_file='reference_data\refdata_ykj_slam_100.mat';  %Open/Forested and
Wooded density
savefile=['results_nagler\TR_variation_split_areas\',hakemisto,num2str(TR),
'_',ref_image,'_',mode,'_SCA_results.mat']; %Output

load(slam_file);
load(image_1);


    if strcmp(mode,'forested')   %selection of forested pixels
        s=3;
        f=7;
    end

    if strcmp(mode,'opened')   %selection of open pixels
        s=2;
        f=2;
    end

    if strcmp(mode,'combined')  %selection of both
        s=2;
        f=7;
    end


for y=1:6004
  for x=1:7004
        if(slam_100(y,x)<s) || (slam_100(y,x)>f) %put 0 non interesting
pixels
          sigma0_image(y,x)=0;
        end
  end
end

clear slam_100;
```

```
x=find(sigma0_image);      %Returns the linear indices corresponding with
nonzero data
kuva_SCA=sigma0_image(x);  %Save all nonzero data in a new image
(Kurva_SCA)
clear sigma0_image;        %Free memory

[final_size,turha]=size(kuva_SCA);
load(image_ref);
kuva_ref=sigma0_image(x); %take out all the needed pixels from the
reference image
clear sigma0_image;

for i=1:final_size      %Nagler Method for each pixel

  if (kuva_SCA(i)==0) || (kuva_ref(i)==0) %Non valid data
    kuva_SCA(i)=-99;
  end

  if kuva_SCA(i)~=-99
    if (kuva_SCA(i)/kuva_ref(i)) < (Limit) %Comparing to Threshold level
      kuva_SCA(i)=1;
    else
      kuva_SCA(i)=0;
    end
  end

end

clear kuva_ref;

load(valuma_file);          %load the information about the drainage basins
ref2=valuma_100(x);
clear valuma_100 x;

SCA_estimate(1:Alueita)=0;
pixels_basin(1:Alueita)=0;

for i=1:final_size                  % Go through the whole image
  if (kuva_SCA(i)~=-99) && (ref2(i)~=0)
    alue=ref2(i);
    SCA_estimate(alue)=SCA_estimate(alue)+kuva_SCA(i); %add the value of a
correct pixel
    pixels_basin(alue)=pixels_basin(alue)+1;
  end

end

for alue=1:Alueita
  if(pixels_basin(alue)>Pixels) %check if there are enough pixels
    SCA_estimate(alue)=SCA_estimate(alue)/pixels_basin(alue); %average to
estimate the SCA for the Drainage Basin
  else
    SCA_estimate(alue)=-99;
  end
end
save(savefile,'SCA_estimate','pixels_basin');
```

Appendix II Comparison between the Generated Maps

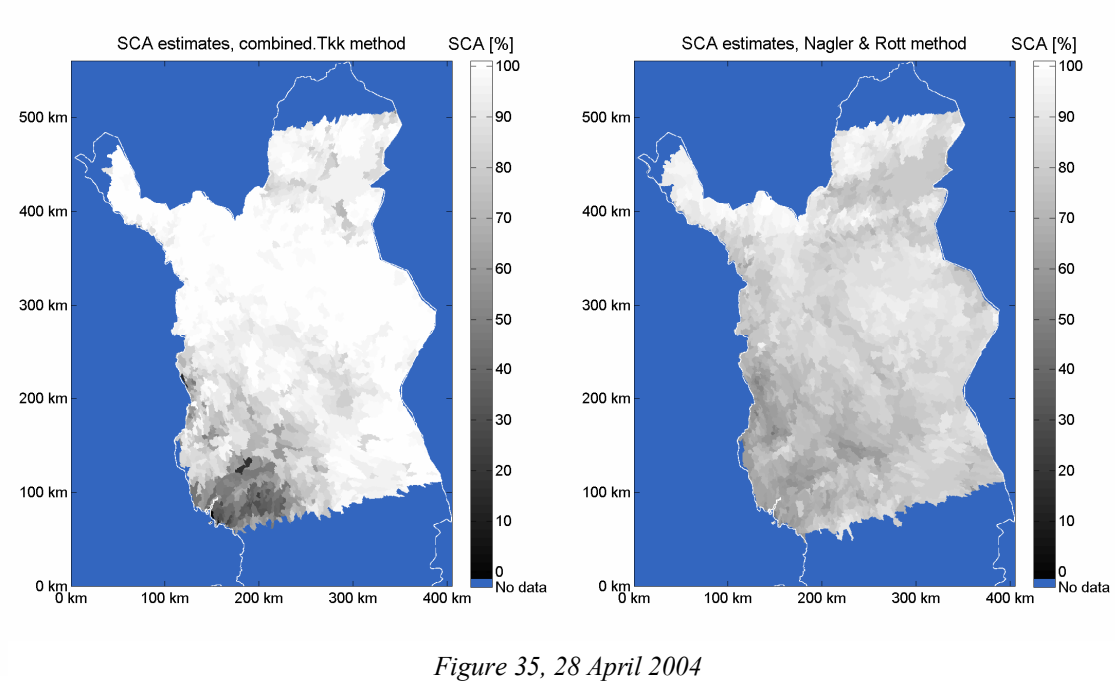

Figure 35, 28 April 2004

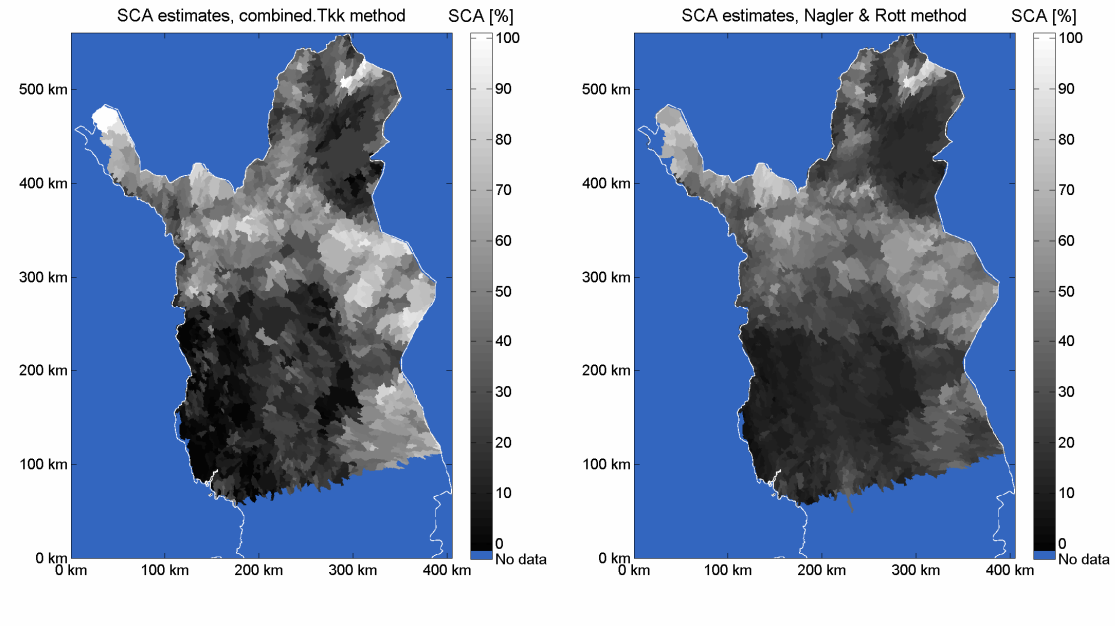

Figure 36, 05 May 2004

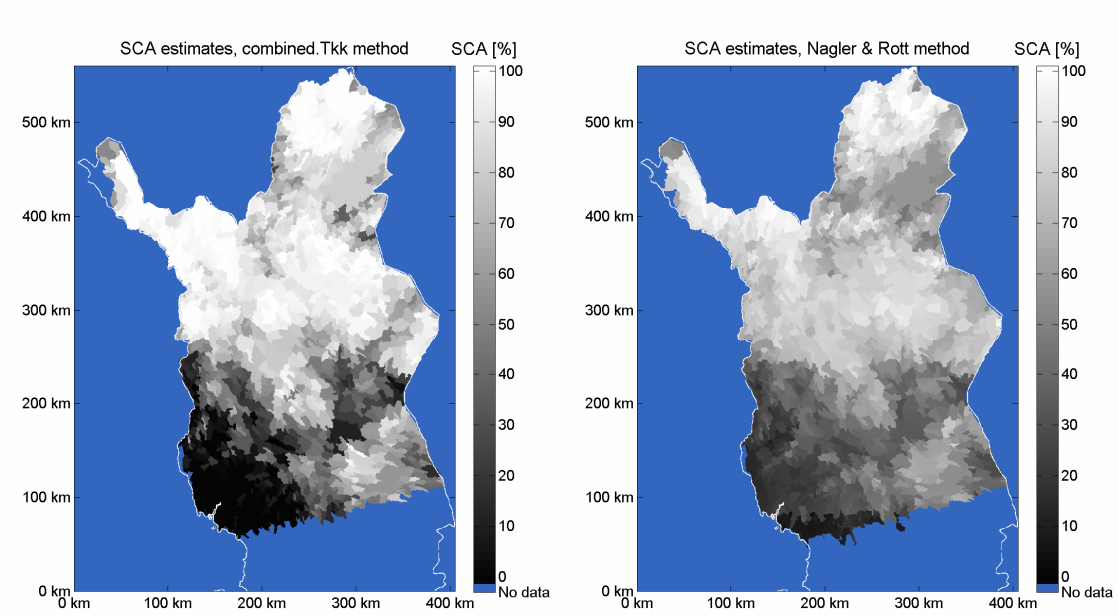

Figure 37, 14 May 2005

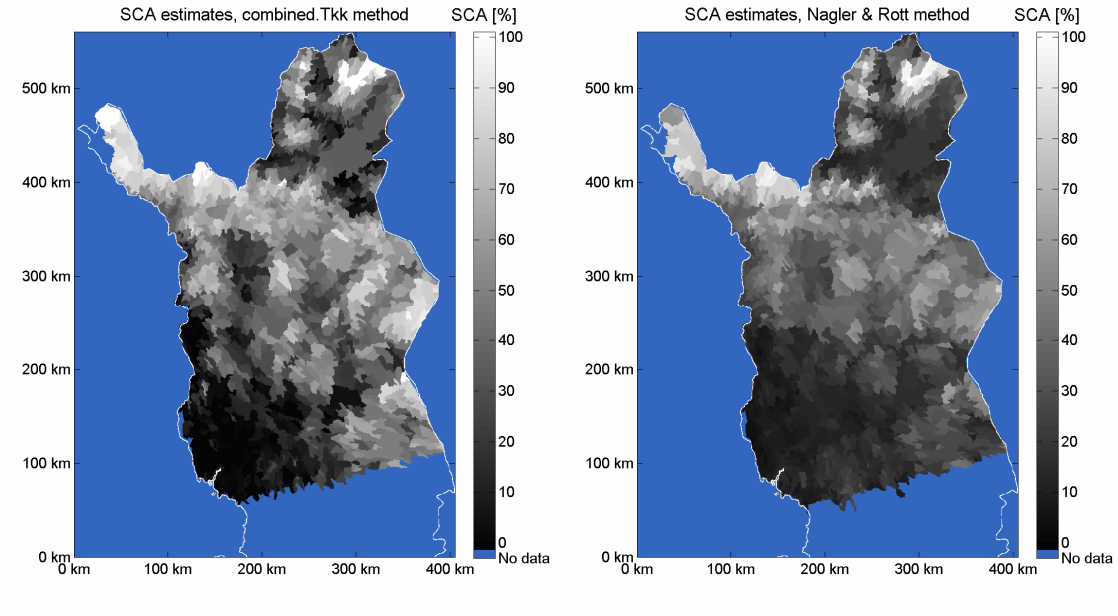

Figure 38, 02 May 2006

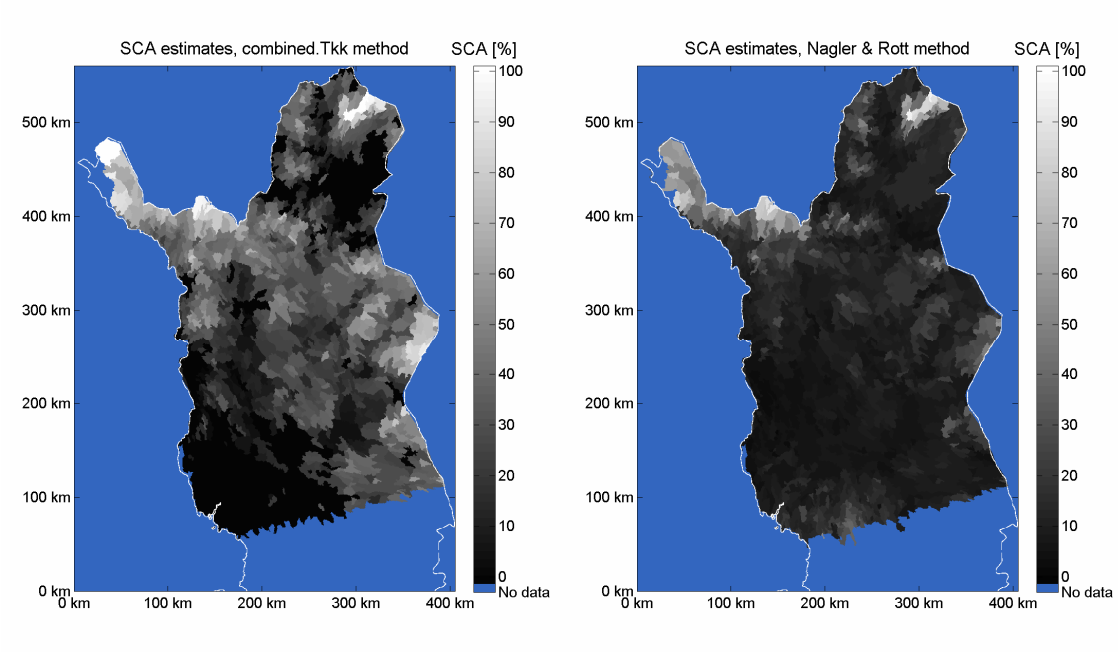

Figure 39, 05 May 2006

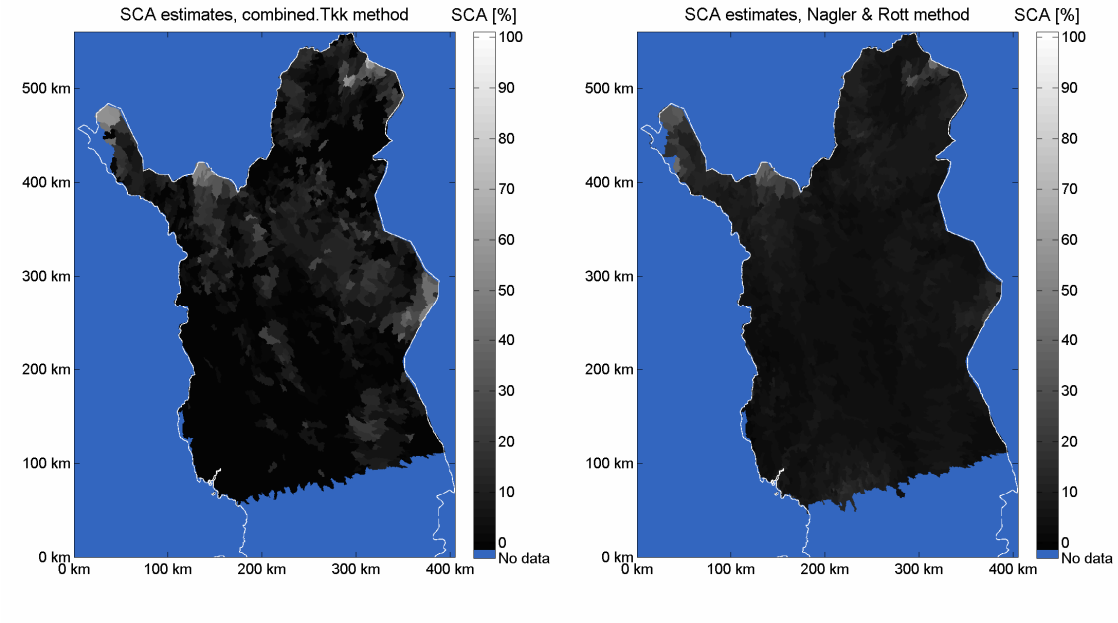

Figure 40, 09 May 2006